"AUREL VLAICU" UNIVERSITY OF ARAD
FACULTY OF FOOD ENGINEERING, TOURISM AND ENVIRONMENTAL PROTECTION
CHEMICAL AND TECHNOLOGICAL RESEARCH CENTER

# Scientific and Technical Bulletin

## Series CHEMISTRY, FOOD SCIENCE & ENGINEERING

**CHEMICAL CHARACTERIZATION OF SOME COMMERCIALLY AVAILABLE TEA TREE OILS (pages 21-27)**

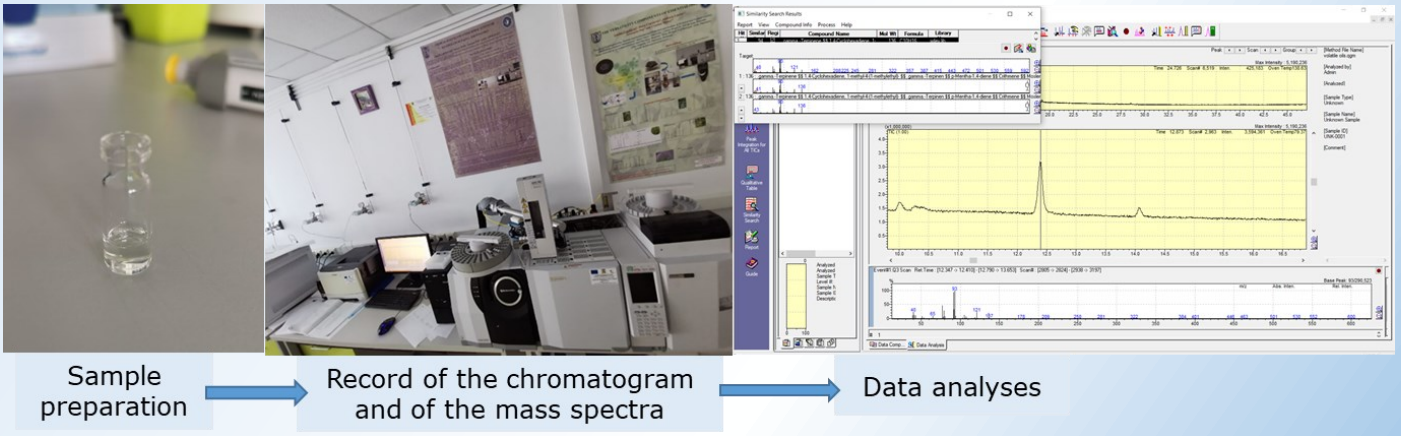


**Year XIX, Vol. 18, 2021**

**https://www.uav.ro/jour/index.php/stb-cfse/index**

**“AUREL VLAICU” UNIVERSITY OF ARAD**

**FACULTY OF FOOD ENGINEERING, TOURISM AND ENVIRONMENTAL PROTECTION**

**CHEMICAL AND TECHNOLOGICAL RESEARCH CENTER**

# Scientific and Technical Bulletin

## Series CHEMISTRY, FOOD SCIENCE & ENGINEERING

**Year XIX, Vol. 18, 2021**

**ISSN 1582-1021**

**e-ISSN 2668-4764**

EDITURA UNIVERSITĂȚII
AUREL VLAICU
A R A D

EDITURA UNIVERSITĂȚII
AUREL VLAICU
A R A D

# CONTENTS

**3** COMPARATIVE STUDY OF THE CHELATING AGENTS INFLUENCE ON THE WEIGHT LOSS OF COTTON FABRICS DURING ENZYMATIC SCOURING
Mihaela DOCHIA, Nicolae DINCĂ, Simona GAVRILAȘ

**10** FT-IR CHARACTERIZATION OF CELLULOSE CRYSTALLINITY FROM RAW BAST FIBERS
Dorina Rodica CHAMBRE, Mihaela DOCHIA

**18** SENSORY CHARACTERISTICS OF YOGHURT FORTIFIED WITH KIWANO FRUIT
Mihaela MEȘTER, Anca Mihaela DICU, Daniela DIACONESCU, Monica ZDREMȚAN, Dumitru CONDRAT

**21** CHEMICAL CHARACTERIZATION OF SOME COMMERCIALLY AVAILABLE TEA TREE OILS
Maria-Daniela MOT, Nicoleta MIHOC, Andreea Ioana LUPITU, Cristian MOISA, Adina Maria BODESCU, Lucian COPOLOVICI, Dana Maria COPOLOVICI

**28** GREEN SYNTHESIS AND CHARACTERIZATION OF SILVER NANOPARTICLES OBTAINED FROM THYMUS VULGARIS L. HYDROLAT
Alina CIUREL, Andreea LUPITU, Lucian COPOLOVICI, Cristian MOISA, Dana COPOLOVICI

**34** FATTY ACIDS PROFILE OF SOME COMMERCIALLY FISH ROE
Carmen POPA, Iulia TIMOFTE, Lucian COPOLOVICI, Dana Maria COPOLOVICI

**ADDRESS**
Faculty of Food Engineering, Tourism and Evironmental Protection,
„Aurel Vlaicu" University, Elena Dragoi St., Nr. 2, L31, Arad, Romania
Phone: 0040257369091
*E-mail:* dana.copolovici@uav.ro

**Scientific and Technical Bulletin, Series: Chemistry, Food Science and Engineering is covered/indexed/abstracted in:**

| | |
|---|---|
| Directory of Research Journals Indexing | **Directory of Research Journals Indexing** |
| ROAD | **Directory of Open Access Scholarly Resources** |
| OCLC WorldCat | **World Cat** |
| Google Scholar | **Google Scholar** |
| CABI | **CABI** |
| INDEX COPERNICUS INTERNATIONAL | **Index Copernicus International** |

*ARTICLE*

# COMPARATIVE STUDY OF THE CHELATING AGENTS INFLUENCE ON THE WEIGHT LOSS OF COTTON FABRICS DURING ENZYMATIC SCOURING

**Mihaela DOCHIA[1], Nicolae DINCĂ[2], Simona GAVRILAȘ[2,]***

*[1] Research Development Innovation in Natural and Technical Sciences Institute, "Aurel Vlaicu" University of Arad, Romania, 2 Elena Drăgoi, Arad, 310330, Romania*
*[2] Faculty of Food Engineering, Tourism and Environmental Protection, "Aurel Vlaicu" University of Arad, Romania, 2 Elena Drăgoi, Arad, 310330, Romania*
*[*]Corresponding author email: simona.gavrilas@uav.ro*

***Abstract:*** *The proposed study offers an alternative to classical cotton fabrics scouring treatment. It is based on reagents and process utilization with low environmental impact. The experimental design studies the weight loss of cotton fabric during enzymatic scouring in ultrasound media due to the variation of two independent factors at five levels: enzyme concentration weight over fiber (1, 1.3, 2, 2.7, and 3 %) and treatment time (15, 21, 35, 49 and 55 min.), using two complexing agents individually (EDTA or sodium citrate at 2g/L). The weight loss of cotton fabric (dependent variable) was expressed in the percentage from the initial weight. The polynomial equations obtained by multiple regression analysis indicate that the influence of the two factors on the studied intervals decreases in order: time>enzyme concentration when EDTA is used, and vice versa in the case of sodium citrate. In the studied intervals of the variables, the weight loss varies between 0.43-2.40 % in the EDTA version and 0.77-1.79 % in the sodium citrate version. Response surface graphics for the two variants of complexants show how much enzyme concentration and time can be reduced in the process to obtain a suitable scouring treatment. Analyzing the obtained results, we consider sodium citrate a viable alternative for bioscouring from technological and environmental aspects.*

**Keywords**: bioscouring, chelating agents, pectinases, multiple regression analysis, optimization.

## INTRODUCTION

There were considered the aspects regarding the environment, costs, and fiber structural damages. Green approaches to classical industrial processes and technologies are continually developed in the last decade. This trend is well represented also in the textile industry, known as environment and human health harmful due to the high quantity of chemicals present in the wastewaters. (Dey et al. 2015, Sarayu et al. 2012, Djehaf et al. 2017). Thus, in the finishing of the cotton, the simple step of samples washing in boiling water facilitates the pectinases access to the substrate, thus contributing to the increase of the hydrolysis reaction yield (Wang et al. 2007). The same principle is also based on the influence of ultrasound (US) on the bioscouring treatment (Erdem et al. 2018). Due to the cavitation effect, the diffusion of enzyme molecules in the textile substrate is improved by using ultrasound energy, shortening the reaction time and the amount of enzyme used (Yachmenev et al. 2002).

An eco-friendly vision should involve all industrial processes. This perspective is found in the fabrics manufacturing units. The concern for cleaner treatments is present from the first steps, meaning scouring.

It is an important preparative phase step in the technological flow. It assumes removing different noncellulosic attendants (wax, dust, pigments, pectin, lignin) on the natural fibers. Many studies underline the possibility of successfully replacing the alkaline scouring treatment with the enzymatic one.

For cotton, single or combined enzymes were used to hydrolyze the pectin (Rajulapati et al. 2020, Shanmugavel et al. 2018, Hebeish et al. 2009) or polymerized esters of different fatty acids and pectin (Hong et al. 2019). After such treatment, the fabrics' technical parameters were comparable (Rajulapati et al. 2020) or improved compared with the classical treatment (Shanmugavel et al. 2018).

For bioscouring treatment, pectinases were found to be the most effective. So far, many studies have been done with different

pectinases to optimize cotton scouring. In the beginning, one disadvantage was the prolonged treatment time, but the development of new pectinases and auxiliaries made the process more feasible for industrial-scale application (Madhu and Chakraborty 2017).

In the pretreatments of cellulosic fabrics, besides enzymes, the complexing and sequestering agents like EDTA are used to bind $Ca^{2+}$ ions and enhance the efficiency of enzymes, to accelerate the removal of non-cellulosic impurities from the textile support (Csiszár et al. 2001, Hebeish et al. 2012). EDTA has a high affinity for most of the metal ions but is a non-biodegradable compound, and the activity of some enzymes like pectate lyases depends on the amount of calcium ions; thus, the effectiveness of the bioscouring could be affected by the total removal of $Ca^{2+}$ ions (Chiliveri and Linga 2014).

Various approaches with promising results on the use of sodium citrate as a complexing agent in the bioscouring treatment of cellulosic and lignocellulosic fabrics have been developed by Dochia et al. Sodium citrate is an eco-friendly biodegradable complexing agent that could successfully replace EDTA in the bioscouring process (Dochia et al. 2016, Dochia et al. 2018a, Dochia et al. 2018b).
The fabric weight loss was one of the parameters evaluated to establish the bioscouring efficiency, as a difference before and after the treatment.

It is a significant factor because it indicates the overall degradation impact of the applied treatments and is relevant for subsequent finishing operations influencing the fabric's quality, comfortability, and other properties (Bahrum Prang Rocky 2012).

The purpose of our study was to compare the effects of the two chelating agents (EDTA and sodium citrate) on the weight loss of cotton fabrics and to establish the best experimental conditions for bioscouring treatments using mathematical models and response surface methodology (RSM).

## MATERIALS AND METHODS

### *Materials*

For the bioscouring treatment, 100% cotton fabric was used. The technical specifications were the follows 150±3 cm width and 200±10 g/m$^2$ weight, 25/2 Ne (Number English) on warp yarns, and 25/1 Ne on weft yarns.

The enzymatic treatment bath contained: Beisol PRO, a commercial pectinases mixture, and the Denimcol Wash RGN surfactant purchased from CHT Benzema. Sodium citrate (monosodium citrate, CAS: 18996-35-5) and EDTA (ethylenedinitrilotetraacetic acid-disodium salt, CAS: 6381-92-6) were provided by Sigma-Aldrich.

### *Methods*

*Cotton fabrics pretreatment*

Naturally, cotton fabrics have physically bind impurities that need to be removed before the specific technological treatments. In this regard, the samples were subjected to water washing in an AATCC standardized Lander-Ömeter, model M228-AA from SDL Atlas Company-USA at 100°C, followed by room temperature drying. For the conditioning of the samples, the drying method (water evaporation) of the samples was used until a constant mass was obtained. For this, the Sartorius MA 100 balance was utilized.

*Bioscouring treatment*

The reaction was developed in an ultrasound media at 45 kHz. A 1:20 fabric to liquid ratio was used. The enzymatic product content in the treatment bath varied between 1-3% (1, 1.3, 2, 2.7, and 3 % o.w.f.), and the hydrolysis time was between 15-55 min (15, 21, 35, 49, and 55 min.), at 55°C (see Table 1).

There were also used 2g/L of complexing agents: monosodium citrate (~10 mmol·L$^{-1}$) or EDTA(~ 5 mmol·L$^{-1}$) and 0.5% surfactant (Denimcol Wash RGN). The reason for using two different molar concentrations of complexing agents was explained in a previous paper (Dochia et al. 2018).

The pectinases were inhibited after the time expired, keeping the samples for 15 min. in hot water at 80°C. Then, they were washed several times with cold distilled water, dried at room temperature, and afterward weighed after drying at 105 $^o$C until constant mass in a Sartorius MA100 balance.

*The weight loss determination*

The weight loss evaluation was done using the modified IS:1383-1977 standard. To avoid the influence of water absorbed from the atmosphere, the samples were dried at 105 $^0$C until constant mass in a Sartorius MA100 balance. The results were obtained based on gravimetric determinations and the percentage of weight loss was calculated according to equation (1):

$$\%\text{weight loss}=(W1-W2)\times 100/W1 \quad \textbf{(1)}$$

where: W1, W2 - dried samples fabric weights before and after bioscouring.

The calculated values represent the amount of non-cellulosic attendants (pectin) removed from the fabrics after bioscouring treatment.

***Design of experiments (DOE)***

A fractional factorial experiment, with two independent variables, $X_1$ (enzyme concentration) and $X_2$ (treatment time), using a variable-centered approach at five variation levels, was used to study their effect on the weight loss of cotton (dependent variable) during enzymatic scouring in ultrasound media. Two variants of the process were used, one with EDTA and another with sodium citrate (SC) as chelating agents. The variable values, $X_1$ and $X_2$, and corresponding encodings, $x_1$ and $x_2$, are presented in Table 1.

**Table 1.** Independent variable values of the process, the corresponding levels, and their codification

| | | Independent variables | |
|---|---|---|---|
| | Cod | Enzyme conc. (% o.w.f) | Time (min.) |
| | $x_i$ | $X_1$ | $X_2$ |
| Level | -1 | 1 | 15 |
| | -0.7 | 1.3 | 21 |
| | 0 | 2 | 35 |
| | 0.7 | 2.7 | 49 |
| | 1 | 3 | 55 |

*Data analysis*

The multiple regression procedure and analysis of variance (ANOVA) from MS Excel 2019 software was used (Home Page of Excel 2019). The codified and experimental data (Table 2) were fitted to a polynomial model and

regression coefficients were obtained. The generalized polynomial model used for establishing the importance and interaction of the studied factors was as follows:

$$Yi = \beta_0+\beta_1x_1+\beta_2x_2+\beta_{12}x_1x_2+\beta_{11}x_1^2+\beta_{22}x_2^2 \quad \textbf{(2)}$$

Where: $Yi$ is predicted response, $\beta_0$ is intercept, $\beta_1$, $\beta_2$, $\beta_{11}$, *and* $\beta_{22}$ are linear and quadratic effect terms, and $\beta_{12}$ is interaction effects.

## RESULTS AND DISCUSSIONS

***Yi data analysis***

ANOVA of *Yi* series of experimental values, corresponding to the variants with EDTA and SC (Tabs. 2 and 4), show that they differ significantly (hypothesis $H_1$). Both the *Fischer* test and the *P-value* confirm this hypothesis:

$$F = 3.63 > 2.60 = F_{crit}$$

$$P\text{-}value = 0.014 < 0.05$$

Consequently, enzyme concentration and treatment time are significant factors for cotton's ultrasonic enzymatic scouring process using EDTA and SC complexing agents.

***Fitting the model***

The multiple regression equation obtained with MS Excel 2019 is an empirical relationship between the weight loss of cotton (% from the initial weight) and the two factors in coded units. The significance of each coefficient was appreciated using the *Student t-test* and *P-value*. The corresponding variables will be more significant if the absolute *t-Stat* value is larger or the *P-value* is smaller (Home Page of NIST/SEMATECH, 2013). The fractional factorial experiment and the results for the two variants of complexing agents are mentioned in Tables 2 and 4.

**Table 2.** Fractional DOE for EDTA variant, the observed responses, and predicted values for weight loss of cotton fabric

| **EDTA** | Variable levels | | Experimental | Predicted |
|---|---|---|---|---|
| | $x_1$ | $x_2$ | *Yi* (%) | *Yi* (%) |
| 1 | -0.7 | -0.7 | 0.48 | 0.60 |
| 2 | 0.7 | -0.7 | 0.59 | 0.70 |
| 3 | -0.7 | 0.7 | 0.64 | 0.92 |

| | | | | |
|---|---|---|---|---|
| 4 | 0.7 | 0.7 | 1.63 | 1.90 |
| 5 | -1 | 0 | 0.51 | 0.65 |
| 6 | 1 | 0 | 1.27 | 1.42 |
| 7 | 0 | -1 | 0.44 | 0.49 |
| 8 | 0 | 1 | 1.75 | 1.57 |
| 9 | 0 | 0 | 1.04 | 1.03 |
| 10 | 0 | 0 | 1.01 | 1.03 |
| 11 | 0 | 0 | 1.01 | 1.03 |
| 12 | 0 | 0 | 1.02 | 1.03 |
| 13 | 0 | 0 | 1.08 | 1.03 |

**Table 3.** Significance of regression coefficients for weight loss of cotton fabric (% from the initial weight) for EDTA variant

| *Coefficients* | | *t Stat* | *P-value* |
|---|---|---|---|
| $\beta_0$ | 1.032 | 18.73 | 3.06983E-07 |
| $\beta_1$ | 0.384 | 6.21 | 0.000440618 |
| $\beta_2$ | 0.540 | 8.72 | 5.21848E-05 |
| $\beta_{12}$ | 0.445 | 3.54 | 0.009425801 |
| $\beta_{11}$ | -0.220 | -2.35 | 0.051318147 |
| $\beta_{22}$ | -0.015 | -0.16 | 0.874465109 |

The coefficients $\beta_{11}$, $\beta_{22}$ , , and their *t-Stat* are small, and their *P-value* is big (Table 3), so the corresponding terms can be neglected. The equation for the EDTA variant becomes:

$$Yi = 1.032+0.384x_1+0.54x_2+0.445x_1x_2 \quad \textbf{(3)}$$

The plus sign of the coefficients indicates a direct action of factors on the weight loss. The action of the factor is stronger if the absolute value of its coefficient is greater. Consequently, the significance of the factors decreases in the order x2>x1 in studied intervals, and there is an interaction between them, x1x2>0 (Table 3).

**Table 4.** Fractional DOE for SC variant, the observed responses, and predicted values for weight loss of cotton fabric

| **SC** | Variable levels | | Experimental | Predicted |
|---|---|---|---|---|
| | $x_1$ | $x_2$ | *Yi* (%) | *Yi* (%) |
| 1 | -0.7 | -0.7 | 0.87 | 1.05 |
| 2 | 0.7 | -0.7 | 0.56 | 0.97 |
| 3 | -0.7 | 0.7 | 0.87 | 0.95 |
| 4 | 0.7 | 0.7 | 1.21 | 1.52 |
| 5 | -1 | 0 | 0.85 | 0.95 |
| 6 | 1 | 0 | 1.52 | 1.30 |
| 7 | 0 | -1 | 0.99 | 0.97 |
| 8 | 0 | 1 | 1.16 | 1.28 |
| 9 | 0 | 0 | 1.01 | 1.13 |
| 10 | 0 | 0 | 1.18 | 1.13 |
| 11 | 0 | 0 | 1.27 | 1.13 |
| 12 | 0 | 0 | 1.16 | 1.13 |
| 13 | 0 | 0 | 1.02 | 1.13 |

**Table 5.** Significance of regression coefficients for weight loss of cotton (% from the initial weight) for SC variant

| *Coefficients* | | *t Stat* | *P-value* |
|---|---|---|---|
| $\beta_0$ | 1.125 | 12.02 | 6.28437E-06 |
| $\beta_1$ | 0.177 | 1.68 | 0.136442878 |
| $\beta_2$ | 0.158 | 1.50 | 0.176812475 |
| $\beta_{12}$ | 0.334 | 1.56 | 0.161691597 |
| $\beta_{11}$ | -0.063 | -0.40 | 0.704594935 |
| $\beta_{22}$ | -0.180 | -1.13 | 0.296410667 |

The coefficients $\beta_{11}$, $\beta_{22}$, and their *t-Stat* are small, and their *P-value* is big (Table 5), so the corresponding terms can be neglected. The equation for the SC variant becomes:

$$Yi = 1.125+0.177x_1+0.158x_2+0.334x_1x_2 \quad \textbf{(4)}$$

The significance of the factors decreases in the order $x_1>x_2$ in studied intervals, and there is an interaction between them, $x_1x_2>0$ (Table 5).
These relations were verified by comparing the experimental values with the calculated values. The correlation coefficients illustrate the agreement of these values: 0.95 for equation **(3)** and 0.69 for equation **(4)**. The accuracy offered by experiments and measurements is better in the case of the EDTA variant than the one with SC. ANOVA also confirms that the series of experimental and predicted values (Tabs. 2 and 4) are similar for both variants (Tab. 6).

**Table 6.** *P-value*>0.05 and $F<F_{crit}$ for the experimental and calculated value series shows the validity of the $H_0$ hypothesis, that the compared series are not different

| *Variant* | *P-value* | *F* | *F crit* |
|---|---|---|---|
| EDTA | 0.659 | 0.199 | 4.260 |
| SC | 0.370 | 0.835 | 4.260 |

### *Analysis of response surfaces*

The relationship between independent and dependent variables is illustrated in a three-dimensional representation of the response surfaces generated by the models for the weight loss of cotton (Myers & Montgomery, 2002). The coordinates of the highest points on the surfaces correspond to the values of the factors that ensure the maximum weight loss of cotton fibers. For the variant with EDTA, the surface in Fig.1 indicates that the maximum ($Y_{max}$=2.40 %)

is reached at a marginal point: enzyme concentration ($X_1$, 3% o.w.f) and temperature ($X_2$, 55°C). This maximum point can be calculated with equation **(3)** for $x_1$=1 and $x_2$=1. For the variant with SC as a complexing agent, the surface from Fig.2 indicates the maximum at $Y_{max}$=1.79% for the same values of independent factors, enzyme concentration ($X_1$, 3% o.w.f) and temperature ($X_2$, 55°C).

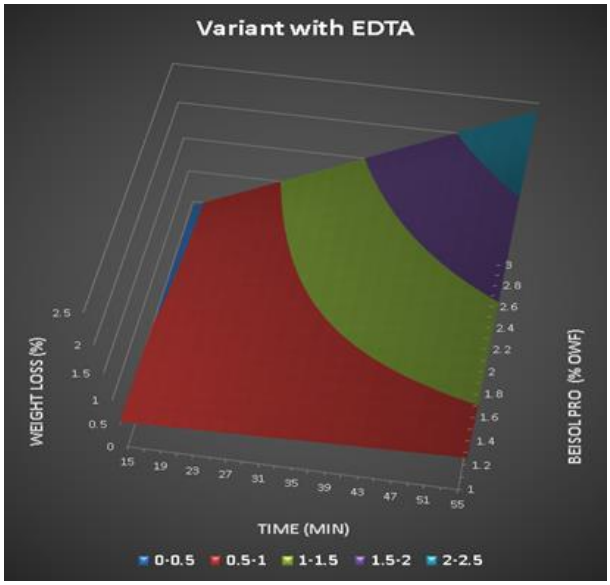


**Fig. 1** Response surface plot (Eq.3) showing the effect of Beisol PRO concentration and treatment time at a constant EDTA concentration (2g/L), on the weight loss of cotton fabrics during enzymatic scouring in ultrasound.

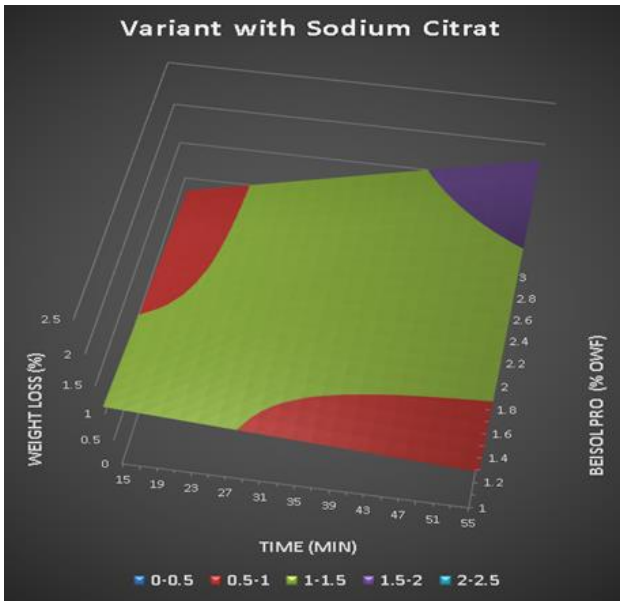


**Fig. 2** Response surface plot (Eq.4) showing the effect of Beisol PRO concentration and treatment time at a constant sodium citrate (SC) concentration (2g/L), on the weight loss of cotton fabrics during enzymatic scouring in ultrasound.

For the minimum weight loss values, the EDTA variant also offers the extreme value, $Y_{min}$=0.43% (for $x_1$=1 and $x_2$=-1) compared to that of the SC variant, $Y_{min}$=0.77 % (for $x_1$=-1 and $x_2$=1).

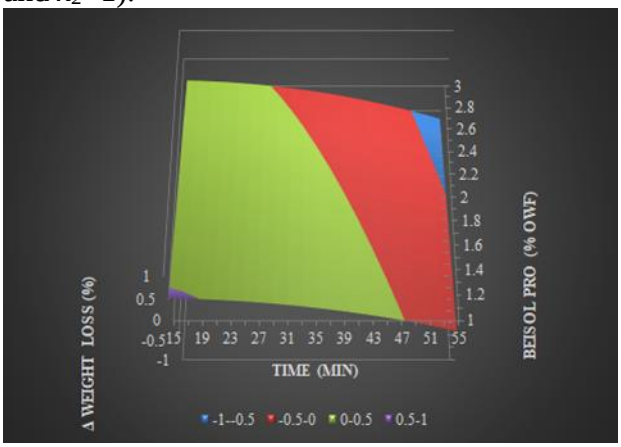


**Fig. 3** Response surface plot (Eq.5) showing the effect of Beisol PRO concentration and bioscouring time on the weight loss difference of cotton fabrics using SC and EDTA complexing agents.

The response surface plot could be used to establish how much Beisol PRO concentration and work time can be reduced to get the desired treatment degree. To optimize the process so that enzymes' Beisol PRO consumption and treatment time is minimal was calculated and represented the response area (Fig. 3) corresponding to the difference regarding weight loss between the variant with SC and the one with EDTA. For this purpose, was used equation **(5)**, that results from multiple regression and ANOVA:

$$\Delta Yi = 0.0931 - 0.2076x_1 - 0.3822x_2 - 0.1647x_1x_2 \quad \textbf{(5)}$$

The green and purple area of the surface indicates positive values of this difference (Fig.3), they are being placed at low values of enzyme concentration and treatment time. This indicates a faster complexation performed by SC than EDTA, thus facilitating easier access of the pectinases to the substrate. The sodium citrate molecules have a lower molecular volume than EDTA and can more easily diffuse into the "egg-box" structure. Also, the diffusion process of complexing agent molecules was favoured by the presence of ultrasound. On the other hand, the enzymatic activity decreases more pronounced with increasing time when using SC compared to EDTA.

## CONCLUSIONS

The multiple regressions and the response surface methodology were successfully used to control the weight loss of cotton fabrics during ultrasound bioscouring. The use of sodium citrate as a complexing agent is a promising alternative to the classical one because it ensures an acceptable degree of complexation in a shorter time with low consumption of the enzyme. In addition, there are natural circuits in which this substance can be integrated for sodium citrate. Considering those the proposed treatment represents a viable eco-friendly option. The experimental design and data processing described herein may constitute an optimal industrial enzymatic scouring treatment management model.

## ACKNOWLEDGEMENTS

*This work was supported by a grant of the Romanian National Authority for Scientific Research and Innovation, CNCS-UEFISCDI, project number PN-II-RU-TE-2014-4-1370, and „Centru de Cercetare în Ştiinte Tehnice şi Naturale-CESTN" co-funded by European Union through European Regional Development Fund Structural Operational Program "Increasing of Economic Competitiveness" Priority axis 2. Operation 2.2.1. POS CCE Nr. 621/2014 POS-CCE.*

## REFERENCES

Bahrum Prang Rocky, A. M. K., 2012. Comparison of Effectiveness Between Conventional Scouring & Bio-Scouring On Cotton Fabrics, IJSER Journal 3(8), ISSN 2229-5518.

Chiliveri, SR, Linga, VR, 2014. A novel thermostable, alkaline pectate lyase from Bacillus tequilensis SV11 with potential in textile industry. Carbohydr Polym 111, 264–272.

Csiszár, E, Losonczi, A, Szakács, G, Rusznák, I, Bezúr, L, Reicher, J, 2001. Enzymes and chelating agent in cotton pretreatment. J Biotechnol 89, 271–279.

Dey, S., Islam, A., 2015. Textile Wastewater Characterization in Bangladesh. Resources and Environment 5(1), 15-44.

Djehaf, K., Bouyakoub, A.Z., Ouhib, R., Benmansour, H., Bentouaf, A., Mahdad, A., Moulay, N., Bensaid, D., Ameri. M., 2017. Textile wastewater in Tlemcen (Western Algeria): Impact, treatment by the combined process. Chemistry International 3(4), 414-419.

Dochia, M, Gavrilaş, S, Pustianu, M, Tomescu, D, Copolovici, DM, 2016. Comparative study regarding the influence of the complexing agents EDTA and sodium citrate on the 50% flax–50% cotton fabrics during the bioscouring treatment. In: Proceedings of 16th international multidisciplinary scientific geoconference SGEM 2016. Book 6, Nano, bio and green-technologies for a sustainable future, conference proceedings 3, 223–230.

Dochia, M., Chambre, D., Gavrilaş, S., Moisă, C., 2018a. Characterization of the complexing agents' influence on bioscouring cotton fabrics by FT-IR and TG/DTG/DTA analysis. Journal of Thermal Analysis and Calorimetry 132, 1489–1498.

Dochia, M., Pustianu, M.,•Moisă, C.,•Chambre, D., Gavrilaş, S., 2018b. Sodium citrate as an eco‑friendly complexing agent for the bioscouring treatment of the cellulosic/lignocellulosic fabrics. Chemical Papers 72, 1881–1888.

Erdem, A., Bahtiyari, I., 2018. Ultrasonic-bioscouring and ozone-based bleaching of cotton slivers and coloration of them with natural dye sources. J. Clean. Prod. 188, 670-677.

Hebeish, A., Hashem, M., Nihal Shaker, N., Ramadan, M., El-Sadek, B., Hady, M.A., 2009. New development for combined bioscouring and bleaching of cotton-based fabrics. Carhydr. Polym. 78, 961-972.

Hebeish, A, Hashem, M, Ramadan, MA, Sadek, B, Abdel-Hady, M, 2012. Bioscouring aided by EDTA and β-cyclodextrin for purification of loomstate cotton and blend fabrics. RJTA 16, 127–138.

Home Page of Excel 2019 can be found under https://support.office.com/en-us/excel.

Home Page of NIST/SEMATECH 2013 e-Handbook of Statistical Methods can be found under http://www.itl.nist.gov/div898/handbook/

Hong, R., Sun, Y., Su, L., Gu, L., Wang, F., Wu, J., 2019. High-level expression of Humicola insolens cutinase in Pichia pastoris without carbon starvation and its use in cotton fabric bioscouring. J. Biotechnol. 304, 10-15.

Madhu, A., Chakraborty, J.N., 2017. Developments in application of enzymes for textile processing, Journal of Cleaner Production 145, 114-133.

Myers, R. H., & Montgomery, D. C., 2002. Response surface methodology: Process and product optimization using designed experiments (2nd ed.). New York: Wiley.

Rajulapati, V., Dhillon, A., Gali, K.K., Katiyar, V., Goyal, A., 2020. Green bioprocess of degumming of jute fibers and bioscouring of cotton fabric by recombinant pectin methylesterase and pectate lyases from *Clostridium thermocellum*. Process. Biochem. 92, 93-104.

Sarayu, K., Sandhya, S., 2012. Current Technologies for Biological Treatment of Textile Wastewater. Appl. Biochem. Biotechnol., DOI 10.1007/s12010-012-9716-6.

Shanmugavel, M., Vasantharaj, S., Yazhmozhi, A., Bhavsar, P., Aswin, P., Felshia, C., Mani, U., Ranganathan, B., Arumugam Gnanamani, A., 2018. A study on pectinases from *Aspergillus tamarii*: Toward greener approach
for cotton bioscouring and phytopigments processing. Biocatalysis and Agricultural Biotechnology 15, 295-303.

Wang, Q., Fan, X.-R., Hua, Z.-Z., Jian Chen, J., 2007. Optimizing bioscouring condition of cotton knitted fabrics with an alkaline pectinase from *Bacillus subtilis* WSHB04-02 by using response surface methodology, Biochem. Eng, J. 34, 107-113.

Yachmenev, VG, Bertoniere, NR, Blanchard, EJ, 2002. Intensification of the bio-processing of cotton textiles by combined enzyme/ultrasound treatment, Chem Technol Biotecnol 77, 559–567.

ISSN 1582-1021
e-ISSN 2668-4764
Edited by "AUREL VLAICU" University
Arad, Romania



10.62591/Scien.Tech.Bull-Chem.FoodSci.Eng.2021.18.01

*ARTICLE*

# FT-IR CHARACTERIZATION OF CELLULOSE CRYSTALLINITY FROM RAW BAST FIBERS

**Dorina Rodica CHAMBRE[1], Mihaela DOCHIA[2*]**

*[1]Faculty of Food Engineering, Tourism and Environmental Protection, "Aurel Vlaicu" University, Romania, 2 Elena Dragoi, Arad 310330, Romania*
*[2]Research Development Innovation in Natural and Technical Sciences Institute, "Aurel Vlaicu" University, Romania, 2 Elena Dragoi, Arad 310330, Romania*
*Corresponding author email: dochiamihaela@yahoo.com*

***Abstract:*** *This paper presents the characterization of native cellulose from the jute, hemp, and flax raw fibers by infrared evaluation of crystallinity ratio (Total Crystallinity Index and Lateral Order Index) and Hydrogen Bond Intensity. The results showed that cellulose from jute fiber has a higher degree of crystallinity while that of hemp fibers has a more ordered structure, with more cellulose chains in a highly organized form. In the flax fibers, the cellulose chains are composed of a larger number of amorphous domains. Hydrogen bond intensity values were influenced by both the ordered cellulose structure and the lignin content of the fibers.*

**Keywords**: bast fibers, native cellulose, infrared crystallinity, hydrogen bond intensity

## INTRODUCTION

The intense development of the synthetic polymer industry in recent years has led to several problems related to the large amount of non-degradable residues accumulated in the environment which have become pollutants in soil and water. This has led to the reconsideration of natural polymers which have become a sustainable and non-polluting alternative in various fields (Mustata et al., 2015).

The lignocellulosic fibers such as hemp, jute, and flax (bast fibers), due to their physicochemical properties and mechanical characteristics, are increasingly used as substitutes for synthetic compounds in various industrial fields. For instance, in the textile industry, the bast fibers are used to obtain a wide range of products, while in the field of automotive or construction materials, they are used as reinforcing agents to obtain biocomposites (Chambre and Dochia, 2020.; Donatelli et al., 2017; Karus and Kaup, 2002; Ouajai and Shanks, 2005). Obtaining quality end-products based on lignocellulosic components is influenced both by the chemical composition of the bast fibers and by the arrangement of the cellulose chains concerning each other (crystallinity) and to the fiber axis (Mustata et al., 2015).

In the chemical composition of bast fibers along with cellulose, which is the major component, there are also some non-cellulosic attendants such as pectin, lignin, hemicelluloses, waxes, etc. which influence the properties and behavior during fibers treatments (Abdel-Halim et al., 2008; Chambre et al., 2019; Ciolacu et al., 2011). While the cellulose consists of crystalline and amorphous domains, in variable proportions (depending on both source and plant variety) the non-cellulosic attendants are amorphous structures. The reactants can penetrate only the amorphous regions with a low ordered structure of cellulosic chains and it is only in these regions and on the surface of the crystallites that the reactions can take place, leaving the crystalline regions unaffected (Ciolacu et al., 2011). Under these conditions, a rigorous evaluation of the crystallinity degree of cellulosic and lignocellulosic materials becomes necessary to obtain quality end-products.

X-ray diffraction (XRD) technique was frequently used to characterize the supramolecular structure of cellulose from fibers and to reveal the modifications that occur after the dissolution/regeneration of cellulose processes (Ciolacu et al., 2011; Eichhorn et al., 2001; Mewoli et al., 2020; Ouajai and Shanks, 2005; Shahzad, 2012).

Nowadays, Fourier Transform Infrared spectroscopy (FTIR) has become a powerful analytical technique to characterize both the changes that occur in the chemical composition of natural textile fibers subjected to various treatments and their crystallinity (Chambre and Dochia, 2018.; Chambre et al., 2019; Ciolacu et al., 2011; Fan et al., 2012; O'Connor et al., 1958; Ouajai and Shanks, 2005). Based on the absorbance values of specific bands, both the crystallinity ratio and the intensity of the hydrogen bonds can be evaluated from the FTIR spectra (Fan et al., 2012; Poletto et al., 2014).

This paper aims to characterize by FTIR ATR spectroscopy some raw bast fibers (hemp, flax, and jute) as well to evaluate the infrared crystallinity ratio through determination of *Lateral Order Index, Total Crystallinity Index,* and *Hydrogen Bond Intensity* values.

## MATERIALS AND METHODS

*Materials*

Raw jute (*Corchorus olitorius*), hemp (*Cannabis sativa*), and flax (*Linum hirsutum*) fibers were taken in the analysis. The jute fibers samples (specific mass: 1.44g/cm$^3$; the average length of elementary fibers: 5mm; average thickness: 18 μm; fineness: 4000 Nm) were purchased from a twine manufacturer in Bucharest. The hemp fiber samples (specific mass: 1.48 g/cm$^3$; the average length of elementary fibers: 22 mm; average thickness: 20 μm; fineness: 4000 Nm) were purchased from a cultivator in north-eastern Romania, while the flax fibers samples (specific mass: 1.50g/cm$^3$; the average length of elementary fibers: 30 mm; the average thickness: 15 μm; fineness: 6000 Nm) were obtained from a fibers processor in Fălticeni. Both flax and jute raw fibers were imported from Asia. Before analysis, the raw fibers were carefully cleaned of mechanical impurities and then conditioned on Sartorius MA 100 system at 105$^0$ C to constant mass. For FT-IR analyzes, the fibers samples were finely chopped.

*Method*

The FT-IR spectra of the fibers were acquired with a Vertex 70 (Bruker, Germany) spectrophotometer equipped with a Pike Miracle ATR cell. The spectral data were recorded on the 600-4000 cm$^{-1}$ wavelength range with a resolution of 4 cm$^{-1}$. A total of 64 scans were taken for each sample. The OPUS 6.5 (Bruker) software was used both for the acquisition and processing of spectra and for the extraction of average spectra of each fiber type. Before each measurement, the ZnSe crystal (fixed at an incidence angle of 45$^0$) of the single reflection horizontal ATR accessory was carefully cleaned with isopropyl alcohol and the background was collected. For each fiber type, the FT-IR ATR measurements were performed in triplicate. The absorbance values ($A$) for the interest bands were evaluated from the vector normalized spectra at the 1314 cm$^{-1}$ band which is assigned to $CH_2$ rocking vibration.

The *infrared crystallinity ratio* was determined by the following methods:

- *Lateral Order Index (LOI)*

$$LOI = \frac{A_{1424}}{A_{897}} \qquad \text{(Eq.1.)}$$

were: $A_{1242}$ is the absorbance value of the band located at ~1424 cm$^{-1}$; $A_{897}$ is the absorbance value of the band located at ~897 cm$^{-1}$

- *Total Crystallinity Index (TCI)*

$$TCI = \frac{A_{1367}}{A_{2920}} \qquad \text{(Eq.2.)}$$

were: $A_{1368}$ is the absorbance value of the band located at ~1367 cm$^{-1}$; $A_{2920}$ is the absorbance value of the band located at ~2920 cm$^{-1}$

The *Hydrogen Bond Intensity (HBI)* by (Eq.3.):

$$HBI = \frac{A_{3337}}{A_{1317}} \qquad \text{(Eq.3.)}$$

were: $A_{3334}$ is the absorbance value of the band located at ~3337 cm$^{-1}$; $A_{1348}$ is the absorbance value of the band located at ~1317 cm$^{-1}$

## RESULTS AND DISCUSSIONS

Hemp, flax, and jute fibers are lingo-cellulosic materials (bast fibers) that are extracted from the stems of plants with the same name. The bast fibers are multicellular and have all the cells with the same structure. The differences between them refer to the external shape, to the dimensions, to the proportion between the chemical components, and some structural

details. The chemical composition (wt% - the percentage of total weight) of the jute, hemp, and flax fibers reported in the literature is shown in Table 1.

**Table 1.** Chemical composition of the bast fibers used in the study

| Fibers | Cellulose (wt%) | Hemicelluloses (wt%) | Lignin (wt%) | Pectin (wt%) | Waxes and extractable substances (wt%) | Ref. |
|---|---|---|---|---|---|---|
| Jute | 45 - 71 | 13 - 20 | 12 - 26 | 0.2 - 10 | 0.5 - 2.5 | (Poletto et al., 2014; Summerscales et al., 2010) |
| Hemp | 74 - 77 | 14 - 21 | 3.7 - 5.5 | 0.9- 1.55 | 4 - 5 | (Chambre and Dochia, 2018.; Manaia et al., 2019; Shahzad, 2012; Väisänen et al., 2018) |
| Flax | 71 - 76 | 17 - 28 | 2.2 - 7.0 | 2 - 5 | 6.5 – 9.5 | (Abdel-Halim et al., 2008; Chambre and Dochia, 2020.; Summerscales et al., 2010) |

From Table 1 it can be noticed that cellulose, hemicelluloses, and lignin are the main components that have an important influence on the chemical, mechanical, physical, and end-use properties of the bast fibers (Poletto et al., 2014; Shamolina et al., 2003). The crystallinity properties of the fibers may be affected by the high content of non-cellulosic attendants which, as is known, have a pronounced amorphous character. In addition, waxes and pectin are responsible for the non-wetting the behaviour of cellulosic and lingo-cellulosic fibers by water, causing several technical problems during the dyeing and finishing processes (Chambre et al., 2019; Choe et al., 2018; Dochia et al., 2018).

Figure 1 presents the FT-IR ATR normalized average spectra (average of three recorded spectra for each type of fibers) of the jute, hemp, and flax raw fibers recorded on 600 - 4000 $cm^{-1}$.

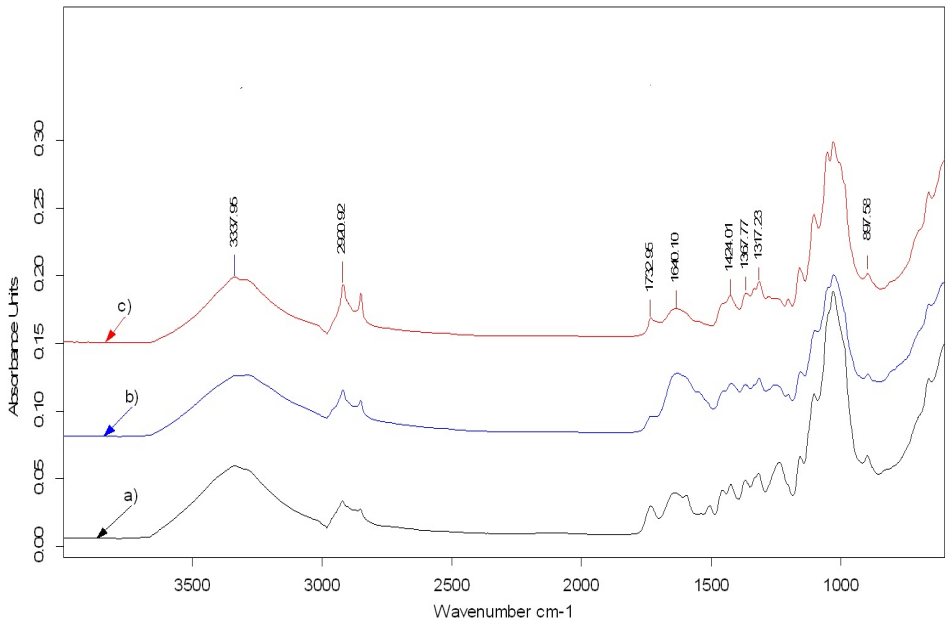


**Figure 1.** FT-IR ATR normalized average spectrum of the bast fibers: a) jute; b) hemp; c) flax

The "fingerprint area" is located between 600 $cm^{-1}$ and 1500 $cm^{-1}$ and contains specific and common bands (Dai and Fan, 2010; Rémy Legrand et al., 2020) of fibers constituents.

The main infrared vibrations as well as the assigned functional groups are presented in Table 2.

**Table 2**. FT-IR absorbance bands (frequency number, $cm^{-1}$) of main constituents from investigated raw fibers

| Assigned functional groups (vibration) | | | | Frequency number ($cm^{-1}$) | | | Ref. |
|---|---|---|---|---|---|---|---|
| Cellulose | Hemicellulose | Lignin | Pectin | Jute fibers | Hemp fibers | Flax fibers | |
| OH stretching vibration; the intramolecular hydrogen bond of O(3)H--O(5), O(2)—O(6) intermolecular hydrogen bond of O(6)H—O(3) in cellulose I | | | | 3337<br>3285 | 3334<br>3287 | 3337<br>3288 | (Bakri and Jayamani, 2016; Ciolacu et al., 2011; Dai and Fan, 2010; Donatelli et al., 2017; Mustata et al., 2015; Shamolina et al., 2003) |
| C-H symmetrical stretching (2900 $cm^{-1}$) | C-H symmetrical stretching | C-H stretching in aromatic methoxyl group and methylene group | C-H symmetrical stretching | 2921 | 2918 | 2920 | |
| | $CH_2$ asymmetric stretching | $CH_2$ asymmetric stretching | $CH_2$ asymmetric stretching | 2850 | 2851 | 2849 | |
| | Stretching vibration of acetyl and uronic ester groups attached to hemicelluloses (1740 $cm^{-1}$) | Conjugate C=O groups of hydroxycinnamic acids | C=O stretching from carboxyl and ester groups of polygalacturonic acid | 1732 | 1730 | 1731 | |
| | O-H bending vibration principally related to the presence of water in hemicellulose | | Symmetric and asymmetric stretching of $COO^-$ from $Ca^{2+}$ pectate | 1642 | 1639 | 1640 | |
| | | C=C aromatic symmetrical stretching and polyphenolic groups vibrations | | 1595<br>1505 | - | - | |
| HCH bending of crystalline cellulose | C-H bending and OCH in plane bending vibration | | | 1424 | 1424 | 1425 | |
| C-OH in plane bending | | | | 1367 | 1367 | 1366 | |
| $CH_2$ rocking vibration at C6 in cellulose I and cellulose II | | | | 1317 | 1316 | 1317 | |
| | | C-O, C-C, C=O and G ring stretching in lignin | | 1248 | 1245 | 1246 | |
| C-O-C symmetric stretching of cellulose, O-H plane deformation | C-O-C symmetric stretching of hemicellulose | | | - | 1203 | 1202 | |
| Asymmetrical bending of C-O-C group of amorphous cellulose | | | | 1157 | 1156 | 1159 | |
| | C-O and C-C stretching band of xylanes and C-O-C stretching of the glycosidic linkage | | | 1054 | 1054 | 1057 | |
| | Aromatic C-H in plane deformation and C-O stretching | Aromatic C-H in plane deformation and C-O stretching of lignin | | 1030 | 1038 | 1029 | |
| C-H bending of amorphous cellulose | | | | 897. | 896. | 897 | |
| C-C-O, C-O-C stretching of β-(1→4)- glycosidic linkages | | | | | | | |
| C-OH out-of-plane bending | | | | 661 | 660 | 661 | |

The wide bands observed at ~ 3337 $cm^{-1}$ and ~ 3287 $cm^{-1}$ can be correlated with the stretching vibration of groups (OH) in polysaccharides (Donatelli et al., 2017; Poletto et al., 2014) . The (OH) groups can be associated, by hydrogen bonds, both intra-, and inter-molecular as well as with adsorbed water molecules. In cellulose, the hydrogen bond associations are distributed both in crystalline and amorphous domains and it is possible to establish a relation between the OH-bands and the cellulose structure (Fan et al., 2012). According to the Gardner-Blackwell model, reported in the literature by some authors (Fan et al., 2012), hydrogen bonds for cellulose I include two intra-molecular bonding (O(2)H---O(6) and O(3)---O(5)) and one inter-molecular bonding (O(6)---O(3)) recorded between 3350 $cm^{-1}$ and 3230 $cm^{-1}$.

The bands recorded at ~2920 $cm^{-1}$ and ~ 2850 $cm^{-1}$ can be associated with the (C-H) and ($CH_2$) symmetric and asymmetric stretching vibration from fibers components (Rémy Legrand et al., 2020). The literature mentions that the stretching vibration of (CH) for cellulose occurs at 2900 $cm^{-1}$ and the presence of amorphous non-cellulosic attendants leads to the recording of two extra intense bands, one shifted to a higher value of wavenumber and the other one to a smaller value.(Chambre and Dochia, 2020.; Ciolacu et al., 2011; Rémy Legrand et al., 2020; Shamolina et al., 2003). So, for the investigated bast fibers the two bands recorded on 3000-2800 $cm^{-1}$ range can be associated with the presence of pectin, waxes, and hemicelluloses. According to Table 1 data, the intense bands observed in the spectra of flax fibers at ~ 2920 $cm^{-1}$ and ~ 2850 $cm^{-1}$ are due to the presence of a higher content of pectin and waxes.

Absorption band located at ~1730 $cm^{-1}$ corresponds to (C=O) symmetric stretching from carboxylic or ester groups of polygalacturonic acid from pectin with a small contribution of the acetyl groups from uronic esters attached to hemicelluloses and of the conjugate carbonyl groups of hydroxycinnamic acids from lignin (Chambre and Dochia, 2018., 2020.; Chambre et al., 2019; Donatelli et al., 2017). The intense absorption band located at 1732 $cm^{-1}$ in the jute fibers spectrum confirms the higher content of pectin.

The peak recorded at ~1505 cm $cm^{-1}$ and ~ 1595 $cm^{-1}$ are specific to carbon double bond (C=C) and the vibrations of polyphenolic groups of lignin (El-Abbassi et al., 2020; Wang et al., 2019). Another specific band for lignin can be observed at ~1248 $cm^{-1}$ and corresponds to C-O, C-C, C=O, and G ring stretching vibrations (Abdel-Halim et al., 2008; Donatelli et al., 2017; El-Abbassi et al., 2020).

The peak centered at ~1424 $cm^{-1}$ is assigned to asymmetric ($CH_2$) bending vibration in cellulose (Choe et al., 2018; Fan et al., 2012; Ouajai and Shanks, 2005; Rémy Legrand et al., 2020). This band is also known as the "crystallinity band", and the decrease in the intensity of this band reflects a decrease in the crystallinity degree of the samples (Ciolacu et al., 2011; Fan et al., 2012; Ouajai and Shanks, 2005).

The peak recorded at ~1367 $cm^{-1}$ can be assigned to in-plane bending of (C-OH) groups from cellulose (El-Abbassi et al., 2020; Poletto et al., 2014; Rémy Legrand et al., 2020) and that one of ~1317 $cm^{-1}$ at bending vibration of ($CH_2$) and (C-OH) groups from cellulose (Poletto et al., 2014; Rémy Legrand et al., 2020). The absorbance of the 1367 $cm^{-1}$ peak is useful to determine the index of crystallinity of the fibers samples. Finally, the small peak located at ~897 $cm^{-1}$ can be assigned to the stretching vibration of β-(1→4) glycosidic linkage of (C-O) groups in cellulose (Ciolacu et al., 2011; Poletto et al., 2014; Rémy Legrand et al., 2020). This band is also known as an "amorphous absorption band" and the intensity of this band increase in the amorphous samples (Ciolacu et al., 2011; Fan et al., 2012; Ouajai and Shanks, 2005).

*Infrared crystallinity ratio (LOI, TCI) and Hydrogen Bond Intensity (HBI)*

The crystallinity ratio determination of the fibers samples using FTIR spectroscopy is a simple method but it is necessary to underline that this method gives only relative values, because the fibers spectrum always contains contributions from both crystalline and amorphous regions (Fan et al., 2012). To calculate the empirical crystallinity index of

cellulose, O'Connor (O'Connor et al., 1958) proposed in 1958 the *Lateral Order Index* (*LOI*) as a ratio between the absorbance values of the bands from 1420 $cm^{-1}$ and 893 $cm^{-1}$ ($LOI = A_{1420} / A_{893}$). These bands are sensitive to the amount of crystalline versus amorphous structure in cellulose and enlargement of these bands reflects a more disordered structure. A few years later, for the same purpose, Nelson and O'Connor (Nelson and O'Connor, 1964a, b) introduced the *Total Crystallinity Index* (*TCI*) as a ratio between the absorbance values of the bands at 1370 $cm^{-1}$ and 2900 $cm^{-1}$ ($TCI = A_{1370} / A_{2900}$ ) to evaluate the infrared crystallinity index.

According to Polleto et al. (Poletto et al., 2014), *TCI* is proportional to the crystallinity degree of cellulose while *LOI* is correlated to the overall degree of order in cellulose.

Taking into consideration the chain mobility of cellulose and bond distance between chains, the *Hydrogen Bond Intensity* (*HBI*) of cellulose is correlated to the degree of crystallinity which reflects the intermolecular regularity, as well as to the amount of bound water (Poletto et al., 2014). From the vector normalized and baseline corrected FT-IR spectra of the investigated bast fibres (triplicate) the absorbance values of the ~1424 $cm^{-1}$, 894 $cm^{-1}$, 1367 $cm^{-1,}$ and 2920 $cm^{-1}$ band were determined and the *LOI* and *TCI* were calculated with (Eq1.) and (Eq2.). The ratio between the absorbance bands at 3400 and 1320 $cm^{-1}$ was used to study the *HBI* of the fibers. The obtained results are shown in Table 3.

**Table 3.** Infrared crystallinity ratio and hydrogen bond intensity for the investigated bast fibres

| Fibres | Infrared crystallinity ratio | | Hydrogen bond intensity (*HBI*) |
|---|---|---|---|
| | *(LOI)* | *(TCI)* | |
| Flax | 1.189±0.093 | 0.594±0.102 | 1.084±0.152 |
| Jute | 1.833±0.158 | 0.781±0.088 | 2.250±0.153 |
| Hemp | 2.158±0.108 | 0.648±0.060 | 1.946±0.046 |

Table 3 shows that for the jute and hemp fibers the infrared crystallinity ratio values *LOI* are higher than those obtained for the flax fibers, thus indicating a higher degree of crystallinity and a more ordered cellulose structure. The presence of non-cellulosic attendants (i.e. waxes, hemicelluloses) influences the overall crystallinity of the material. Thus, the high content of amorphous compounds like waxes and extractable substances in flax fibers led to the value of 0.594 for *TCI*, being in accordance with the data reported in the literature by (Kovačević et al., 2012). In addition, the low value for *LOI* (1.189) indicates that the cellulose in the investigated flax fibers is composed of more amorphous regions than in the other two bast fibers.

For hemp fibers, the highest value of *LOI* (2.158) suggests that the cellulose polymer presents more laterally ordered macromolecular chains that allow more intermolecular hydrogen bonds. Comparable values for *LOI* of hemp fibers were reported in the literature by (Ouajai and Shanks, 2005).

According to Poletto et al. (Poletto et al., 2014), a higher cellulose crystallinity of the fibers usually leads to high *HBI* values. This behaviour was observed also for the tree analysed bast fibers. Thus, hemp samples that showed the highest degrees of crystallinity *LOI* also had a higher value for *HBI* (1.946). It should be noted that the *HBI* value reflects both the hydrogen bonds specific to the cellulosic polymer and the hydrogen bonds characteristic of non-cellulosic components. According to Table 1, the jute fibers had the highest content of lignin, which may form intramolecular hydrogen bonds between neighbour phenolic groups. Thus can be explained the highest value obtained for *HBI* (2.250) for the jute fibers even if it does not show the highest overall degree of order in cellulose (*LOI* = 1.833).

## CONCLUSIONS

The characterization of jute, hemp, and flax raw fibers by infrared evaluation of crystallinity ratio (*Total Crystallinity Index* and *Lateral Order Index*) and *Hydrogen Bond Intensity* was done.

The results showed that cellulose from jute fibers has a higher degree of crystallinity (*TCI*) while that of hemp fibers has a higher *LOI* value due to a more ordered structure, with more cellulose chains in a highly organized form. In the flax fibers, the native cellulose chains are composed of a larger number of amorphous domains.

The *TCI* obtained values showed that are strongly influenced by the non-cellulosic attendants content such as waxes from raw fibers while the *HBI* values are influenced by the lignin content.

**ACKNOWLEDGEMENTS**

This work was supported by a grant of the Romanian National Authority for Scientific Research and Innovation, CNCS-UEFISCDI, project number PN-II-RU-TE-2014-4-1370, and „Centru de Cercetare în Științe Tehnice și Naturale-CESTN" co-funded by European Union through European Regional Development Fund Structural Operational Program "Increasing of Economic Competitiveness" Priority axis 2. Operation 2.2.1. POSCCE Nr. 621/2014 POSCCE.

**REFERENCES**

Abdel-Halim, E.S., Fahmy, H.M., Fouda, M., 2008. Bioscouring of linen fabric in comparison with conventional chemical treatment. Carbohydrate Polymers 74, 707-711.

Bakri, M.K., Jayamani, E., 2016. Comparative Study Of Functional Groups In Natural Fibers: Fourier Transform Infrared Analysis (FTIR), pp 167-174.

Chambre, D.R., Dochia, M., 2018. Characterization of alkaline and enzimatically treated hemp fibers by FT-IR ATR spectroscopy. Scien. Tech. Bull-Chem. Food Sci. Eng. 15,, 18-22.

Chambre, D.R., Dochia, M., 2020. Pectin quantification from cellulosic/lignocellulosic raw materials by FT-IR ATR analysis. . Scien. Tech. Bull-Chem. Food Sci. Eng. 17 20-25.

Chambre, D.R., Dochia, M., Gavrilas, S., 2019. TG/DTG analysis of an eco-friendly scoured fabric. Revue Roumaine de Chimie 64, 453-460.

Choe, E.K., Lee, M., Park, K.S., Chung, C., 2018. Characterization of cotton fabric scouring by Fourier transform-infrared attenuated total reflectance spectroscopy, gas chromatography-mass spectrometry and water absorption measurements. Textile Research Journal 89, 2305-2315.

Ciolacu, D., Ciolacu, F., Popa, V., 2011. Amorphous cellulose - Structure and characterization. Cellulose Chemistry and Technology 45, 13-21.

Dai, D., Fan, M., 2010. Characteristic and Performance of Elementary Hemp Fibre. Materials Sciences and Applications 01, 336-342.

Dochia, M., Chambre, D., Gavrilaş, S., Moisă, C., 2018. Characterization of the complexing agents' influence on bioscouring cotton fabrics by FT-IR and TG/DTG/DTA analysis. Journal of Thermal Analysis and Calorimetry 132, 1489-1498.

Donatelli, A., Cuna, D., Tagliente, M., Protopapa, M., Mevoli, A., Aversa, P., Blasi, C., Capodieci, L., Luprano, V.A.M., 2017. Effect of treatments on the aging behaviour of hemp fibres for building construction in the Mediterranean Area. Journal of Building Engineering 11, 37-471.

El-Abbassi, F.E., Assarar, M., Ayad, R., Bourmaud, A., Baley, C., 2020. A review on alfa fibre (Stipa tenacissima L.): From the plant architecture to the reinforcement of polymer composites. Composites Part A: Applied Science and Manufacturing 128, 105677.

Fan, M., Dai, D., Huang, B., 2012. 3 Fourier Transform Infrared Spectroscopy for Natural Fibres. Fourier Transform-Materials Analysis.

Kovačević, Z., Vukušić, S.B., Zimniewska, M., 2012. Comparison of Spanish broom (Spartium junceum L.) and flax (Linum usitatissimum) fibre. Textile Research Journal 82, 1786-1798.

Manaia, J.P., Manaia, A.T., Rodriges, L., 2019. Industrial Hemp Fibers: An Overview. Fibers 7.

Mustata, F., Tudorachi, N., Mustata, A., Mustata, F., 2015. Physical and thermal characterization of some cellulose fabrics as reinforced materials for composite. Journal of Thermal Analysis and Calorimetry 120.

Nelson, M.L., O'Connor, R.T., 1964a. Relation of certain infrared bands to cellulose crystallinity and crystal lattice type. Part II. A new infrared ratio for estimation of crystallinity in celluloses I and II. Journal of Applied Polymer Science 8, 1325-1341.

Nelson, M.L., O'Connor, R.T., 1964b. Relation of certain infrared bands to cellulose crystallinity and crystal latticed type. Part I. Spectra of lattice types I, II, III and of amorphous cellulose. Journal of Applied Polymer Science 8, 1311-1324.

O'Connor, R.T., DuPré, E.F., Mitcham, D., 1958. Applications of Infrared Absorption Spectroscopy to Investigations of Cotton and Modified Cottons: Part I: Physical and Crystalline Modifications and Oxidation. Textile Research Journal 28, 382-392.

Ouajai, S., Shanks, R.A., 2005. Composition, structure and thermal degradation of hemp cellulose after chemical treatments. Polymer Degradation and Stability 89, 327-335.

Poletto, M., Ornaghi, H.L., Zattera, A.J., 2014. Native Cellulose: Structure, Characterization and Thermal Properties. Materials (Basel) 7, 6105-6119.

Rémy Legrand, N.B., Lucien, M.a., Pierre, O., Ebanda, F., Anicet, N., Jean, A., 2020. Physico-Chemical and Thermal Characterization of a Lignocellulosic Fiber, Extracted from the Bast of Cola lepidota Stem. Journal of Minerals and Materials Characterization and Engineering 08, 377-392.

Shahzad, A., 2012. Hemp fiber and its composites - A review. Journal of Composite Materials - J COMPOS MATER 46, 973-986.

Shamolina, I.I., Bochek, A.M., Zabivalova, N.M., Medvedeva, D.A., Grishanov, S., 2003. An investigation of structural changes in short flax fibres in chemical treatment. Fibres and Textiles in Eastern Europe 11, 33-36.

Summerscales, J., Dissanayake, N.P.J., Virk, A.S., Hall, W., 2010. A review of bast fibres and their composites. Part 1 – Fibres as reinforcements. Composites Part A: Applied Science and Manufacturing 41, 1329-1335.

Väisänen, T., Batello, P., Lappalainen, R., Tomppo, L., 2018. Modification of hemp fibers (Cannabis Sativa L.) for composite applications. Industrial Crops and Products 111, 422-429.

Wang, H., Memon, H., Hassan, E., Miah, M., Arshad, M., 2019. Effect of Jute Fiber Modification on Mechanical Properties of Jute Fiber Composite. Materials 12, 1226.

ISSN 1582-1021
e-ISSN 2668-4764
Edited by "AUREL VLAICU" University
Arad, Romania



10.62591/Scien.Tech.Bull-Chem.FoodSci.Eng.2021.18.02

*Scien. Tech. Bull-Chem. Food Sci. Eng., Vol. 18(XIX), 2021, 18-20*

*ARTICLE*

# SENSORY CHARACTERISTICS OF YOGHURT FORTIFIED WITH KIWANO FRUIT

**Mihaela MEȘTER, Anca Mihaela DICU, Daniela DIACONESCU, Monica ZDREMȚAN, Dumitru CONDRAT**

*Faculty of Food Engineering, Tourism and Environmental Protection, "Aurel Vlaicu" University, Romania, 2 Elena Dragoi, Arad 310330, Romania*
*Corresponding author email: mihaelamester@yahoo.com*

***Abstract:*** *Nowadays, the target of food industries is to produce low-calorie products safe for human health. We all know that yoghurt is a popular, flavorful, and healthy dairy product. Due to its high nutritive value, its production and consumption are growing continuously because of its therapeutic properties. To increase attractiveness, we added kiwano pulp in yoghurt, which is rich in antioxidants and vitamins. The nutritional composition of yoghurt and delicious kiwano fruits will lead to a product that will have health benefits and can be consumed by everybody, even by people who suffer from hypercholesterolemia. The sensory evaluation of kiwano yoghurt was performed using the 5-point method. Yoghurt was mixed with 15% fresh fruit pulp. We studied some characteristics: visual (appearance, colour, and consistency), flavour/aroma, and taste. The most appreciated characteristic was the taste. Over 80% of tasters accepted all the sensory characteristics of the analyzed product.*

**Keywords**: yoghurt, kiwano, sensory analysis.

## INTRODUCTION

Yoghurt is a dairy product that has been around for centuries because is easily digested and also is a rich source of proteins, fat, calcium, vitamins, carbohydrates, iron, and phosphorous (Vahedi et al., 2008) and has a special flavor. Over time it has been modified for nutritional benefits, and pleasing flavor, appearance, texture, and aroma.

Lactic acid bacteria in yoghurt include protection against gastrointestinal upsets, enhancing digestion of lactose by maldigestion, decreasing the risk of cancer, lowering blood cholesterol. Also, yoghurt helps the body to assimilate protein, calcium, and iron and improves immune response (Fernandez et all, 2017).

People are interested in functional food obtained by fortification with vegetables and fruits that have healthy and nutritive benefits (Khoulod et al., 2020). As a result, the final product, yoghurt with different vegetables or fruits, is a special food that has functional properties, high nutritional value, and therapeutic effects (McKinley, 2005).

Different fruits are used in yoghurt production (Abdeldaiem, 2019) for making functional fruit yoghurt. In the body's defense system against free radicals, some fruits have important effects (Manisha et al, 2017).

Kiwano (*Cucumis metuliferus*) is rich in antioxidants and vitamins. This exotic fruit is known as African horned cucumber; also goes by horned melon and it tastes like banana and kiwi or passion fruit combined. This fruit boasts an array of vitamins and minerals, many of which play a role in its ability to positively impact health. WHO recognizes the kiwano as an essential fruit that can fight against illness and malnutrition, due to the presence of some valuable nutrients (Bina Rani et al., 2019).

A single kiwano melon (average 200 grams) provides the following nutrients: calories, carbs, protein, fat, vitamin C, vitamin A, vitamin B6, magnesium, iron, phosphorus, zinc, potassium, calcium, copper, and sodium. The African horned cucumber contains high amounts of water (about 88%) and is relatively low in calories, carbs, and fat. About 16% of its calories come from protein - which is relatively high compared to other fruits. The seeds of this fruit contain several antioxidants, including lutein, zinc, and vitamins A, C, and E. The horned melon is low-glycemic and additionally, it's a rich source of magnesium; also is a good source of iron and vitamin C

(Cazanevscaia Busuioc et all, 2020; Šeregelj et all, 2022).

Our aim research is to find out how is been taken by the consumers a new product like this yogurt which has a high nutrition value by adding kiwano pulp.

## MATERIALS AND METHODS

We used the skimmed home-made yoghurt (0.1% fat) with 15% freshly shredded kiwano pulp which was added after fermentation. Kiwano was washed, peeled, and cut into pieces, and seeds were removed. The samples were analyzed immediately after preparation.

The sensory analysis method was the 5-point scaling system. The taster team was formed by 15 members, each one of them accorded from 0 to 5 points for the following three categories: visual (appearance, colour, and consistency), flavour/aroma, and taste.

The steps in the 5 point system: very good – 5 points; good – 4 points; satisfactorily – 3 points; unsatisfactorily – 2 points; bad – 1 point; very bad – 0 points. (Abdalla et al., 2019; Croitoru, 2013; Banu et al., 2002; Dicu, Perța-Crișan, 2012).

## RESULTS AND DISCUSSIONS

The sensory evaluation (Karagul-Yuceer et al, 2007) of kiwano yoghurt was performed using the 5-point method. Yoghurt was mixed with 15% fresh fruit pulp.

In the Table 1 there are the average score points accorded by the tasters to the analyzed characteristics. The average unweighted score was obtained considering the point accorded by each taster for every characteristic and the number of tasters. The average weighted score was calculated in accord with the importance of each sensory characteristic in the global evaluation of the product (for visual - 1.5 factor, for flavour/aroma – 0.5 factor, and taste – 2.0 factor).

**Table 1.** Centralized results obtained from sensory analysis

| **Characteristic /Score** | Visual | Flavour/ aroma | Taste |
|---|---|---|---|
| Average unweighted score | 4.06 | 4.6 | 4.73 |
| Average weighted score | 6.09 | 2.3 | 9.46 |
| **Total average weighted score** | | **17.85** | |

The total average weighted score is 17.85.

Regarding the taste, the tasters had given a high score. For smell the percentage was small and for aspect and consistency, it was higher, as can be seen in Figure 1. In this figure, it can be seen that the most appreciated characteristic was taste.

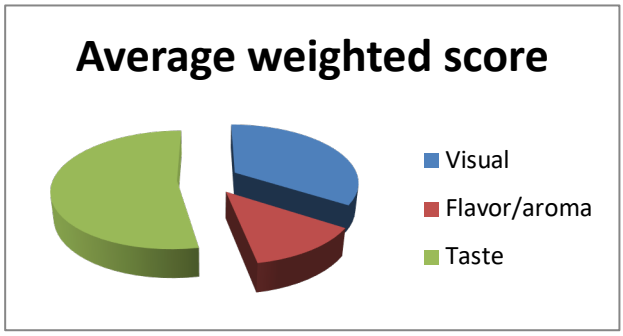


**Figure 1.** The average weighted score for kiwano yoghurt

## CONCLUSIONS

The product has positive and specific sensory characteristics and it was widely accepted by the tasters. The most appreciated characteristic was the taste, followed by flavour/aroma and visual.

On an industrial level, there are no changes, because the process flow is the same as in any other fruit yogurt process.

The shredded kiwano pulp can be used as an ingredient to improve yoghurt sensory, nutritional and physiological qualities.

## REFERENCES

Abdalla, A. K., Ahmed, Z. F. R., 2019. Physicochemical and sensory properties of yoghurt supplemented with green banana flour. Egyptian Journal of Dairy Science 47 (1), 1-9.

Abdeldaiem, A., M., Blassy, Kh., I., 2019. Effect of replacing skim milk powder by sweet lupine powder on characteristics of zebda-

mango 2020 yoghurt drink. Ismailia Journal of Dairy Science and Technology, 6: 9-17.

Banu, C., et all, 2002. Calitatea și controlul calității produselor alimentare, Editura AGIR, București.

Bina, R., Upma, S., Lakha, R., Ravi, S., Harsukh, C., Anju, S. and Raaz, K., Maheshwari, 2019. Incredible Benefits of Exotic Kiwano (Horned Melon) for Wellness, Vigour and Vitality. International Journal of Biological Innovations, 1 (2), 56-59.

Cazanevscaia Busuioc, A., Dediu Botezatu, A.,V., Furdui, B., Vinatoru, C., Maggi, F., Caprioli, G., and Rodica-Mihaela Dinica, R., M. Comparative study of the chemical compositions and antioxidant activities of fresh juices from Romanian Cucurbitaceae varieties, Molecules, 2020, 25(22): 5468.

Croitoru, C., 2013. Analiza sensorială a produselor agroalimentare. Vol. 1, Elemente metrologice, metodologice și statistice, Editura AGIR, București.

Dicu, A., M., Perţa-Crişan, S., 2012, Calitatea şi analiza senzorială a alimentelor. Editura Universităţii „Aurel Vlaicu" Arad, Romania, ISBN 978-973-752-612-0.

Fernandez, M. A., Panahi, S., Daniel, N., Tremblay, A., and Marette, A. Yogurt and Cardiometabolic Diseases: A Critical Review of Potential Mechanisms, Adv. Nutr. 2017 Nov; 8(6): 812–829.

Karagül-Yüceer, Y., Drake, M. A., 2007. Sensory analysis of yogurt. Manufacturing Yogurt and Fermented Milks, 265 - 278.

Khoulod, B., Magdy, O., Amin, G., Mervat H., 2020. Functional Properties of Yoghurt Fortified with Fruits Pulp. Ismailia Journal of Dairy Science & Technology.

Manisha, W. H., Rajak R., Jat D., 2017. Oxidative stress and antioxidants: an overview. International Journal of Advanced Research and Review, 2: 110-119.

McKinley, M. C., 2005. The nutrition and health benefits of yoghurt. International Journal Dairy Technology, 58: 1-12.

Šeregelj, V.; Šovljanski, O.; Tumbas Šaponjac, V.; Vulic, J.; Cetkovic, G.; Markov, S.; Canadanovic-Brunet, J. Horned Melon (Cucumis metuliferus E. Meyer Ex. Naudin) — Current Knowledge on Its Phytochemicals, Biological Benefits, and Potential Applications. Processes 2022, 10, 94.

Vahedi, N., Tehrani, M., M., Shahidi, F., 2008. Optimizing of fruit yoghurt formulation and evaluating its quality during storage. American-Eurasian Journal Agriculture and Environmental Science, 3: 922-927.



10.62591/Scien.Tech.Bull-Chem.FoodSci.Eng.2021.18.03

***ARTICLE***

# CHEMICAL CHARACTERIZATION OF SOME COMMERCIALLY AVAILABLE TEA TREE OILS

**Maria-Daniela MOT[1], Nicoleta MIHOC[2], Andreea Ioana LUPITU[2], Cristian MOISA[2], Adina Maria BODESCU[3], Lucian COPOLOVICI[2], Dana Maria COPOLOVICI[2*]**

*[1] University of Oradea, Doctoral School of Biomedical Sciences, 1 Universitatii St., 410087, Oradea, Romania*
*[2] "Aurel Vlaicu" University, Faculty of Food Engineering, Tourism and Environmental Protection; Institute for Research, Development, and Innovation in Technical, and Natural Sciences, Romania, 2 Elena Dragoi St., Arad, 310330, Romania*
*[3] "Adam Müller Guttenbrunn" High School, 310245, Arad, Romania*
**Corresponding author email: dana.copolovici@uav.ro*

***Abstract:*** *The essential oil obtained from Melaleuca alternifolia is widely used in complementary and alternative medicine due to its antioxidant, antimicrobial, and antifungal activity. The evaluation of the chemical composition of the essential oil available on the market is important especially when allergic potency is reported. The present study evaluated the chemical composition of seven tea tree essential oils by gas chromatography coupled with mass spectrometry. All the analysed samples exhibited a terpinen-4-ol chemotype.*

**Keywords**: essential oils, tea tree oil, GC-MS, chemotype

## INTRODUCTION

Many natural dermato-cosmetic products and alternative medicinal products contain tea tree essential oil (TTO), which is known to have antioxidant capacity (Amarowicz and Pegg, 2019; Hartford and Zug, 2005; Yadav et al., 2017), antimicrobial (Brun et al., 2019; Cox et al., 2001; Melo et al., 2015; Nikolic et al., 2017; Pauli and Schilcher, 2016; Santos et al., 2014; Setzer et al., 2004; Sharifi-Rad et al., 2017), antifungal activity (da Silva et al., 2021; Noumi et al., 2011; Palmeira-De-Oliveira et al., 2009; Sevik et al., 2021), etc. Common examples, which are also available on the market, are: toothpaste, spray and solutions for treating calluses, acne or corns.

TTO is obtained from the leaves of tea tree (*Melaleuca alternifolia*) and is a mobile, colourless to pale yellow, clear liquid with a specific, pleasant odour due to terpenic, coniferous, camphor and mint scent. The yield of the essential oil varies and depends on parameters such as biomass (wild or cultivated shrubs, leaves only or leaves together with terminal parts), variety, chemotype and/or method of production (commercial distillation or preparation by hydrodistillation in the laboratory using a Clevenger apparatus) (Bedini et al., 2020; Borotova et al., 2022; da Silva et al., 2021; de Figueiredo, 2006; de Groot and Schmidt, 2016; Hartford and Zug, 2005; Jammy et al., 2015; Lee et al., 2002; Noumi et al., 2011; Padalia et al., 2015; Sevik et al., 2021).

International Organization for Standardization (ISO) is the worldwide federation of national standards bodies. Certain characteristics of TTO, which belong to the chemotype terpinen-4-ol, are specified for the assessment of its quality. According to ISO, *Melaleuca* essential oil, the chemotype terpinen-4-ol, is obtained by steam distillation of the leaves and terminal parts of the plant *Melaleuca alternifolia* Cheel or *M. linariifolia* Sm (ISO 4730:2017) and should contain more than 30% terpinen-4-ol, 10-28% $\gamma$-terpinene, 5-13% $\alpha$-terpinene, less than 15% 1,8-cineole, less than 12% p-cymene, 1,5-8% $\alpha$-terpineol and small quantities of pinene, terpinolene, limonene, aromadendrene, as determined by gas

chromatography coupled with mass spectrometry: GC-MS (Carson et al., 2006). This chemotype for the TTO is accepted and used in commercial products. There are also other chemotypes for TTO: one terpinolene chemotype, and four 1,8-cineole chemotypes (Carson et al., 2006). The composition of TTO could change during storage, and usually the p-cymene levels increase and $\alpha$- and $\gamma$-terpinene levels decline in time. The stability of TTO is influenced also by light, exposure to air, heat, and moisture so that TTO should be stored in dark, dry, and cool conditions. The oxidation of TTO increased the allergenic potential (de Groot and Schmidt, 2016).

The incorporation of TTO in cream, ointment or gel for topical applications is possible due to its solubility on fats. Topical administration with products containing TTO were well described for diverse pathologies, such as for herpes labialis (Carson et al., 2001; Carson et al., 2008); to treat the ocular itching and ocular demodicosis (Gao et al., 2012); toenail infection; acne (Amer et al., 2020; Avonto et al., 2016); tinea pedis (Braun, 2007). The process of permeation and release kinetics of some TTO marker compounds (1,8-cineole, 4-terpineol and $\alpha$-terpineol) from diverse formulations (creams, ointments, gels) containing TTO was determined (Sgorbini et al., 2017). The results from the study suggests that gels make it possible to use less concentrated formulations with similar local/topical activity as compared with creams or ointments. The authors recommended that the TTO containing formulation as creams could be proposed for cosmetic applications, and gels could be more suitable for dermatological applications (Sgorbini et al., 2017). The inhalation and massage with TTO was reviewed in (Edris, 2007). The main component of the TTO, terpinen-4-ol, was demonstrated to be suitable as novel therapy for treating inflammatory bowel disease (IBD) (Yong et al., 2022).

The aim of our study was to determine the chemical composition of some TTO available on the market.

## MATERIALS AND METHODS

*Essential oils*

Six samples of commercial tea tree essential oils were obtained from the European market and one sample was a gift received from Prof. Ülo Niinemets.

*GC-MS analyses*

Chemical compounds in TTO samples were determined using a gas chromatograph (Shimadzu2010, Kyoto, Japan) coupled with a triple quadrupole mass spectrometer (TQ 8040, Shimadzu, Kyoto, Japan). The column used was an optimal 1MS + WAX column (30 m x 0.25 mm i.d., 0.25 pm film thickness, Macherey-Nagel, Duren, Germany) with helium as carrier gas and a $min^{-1}$ flow of 1 ml. The oven temperature was initiated at 70 °C for 11 min and raised to 190 °C at a rate of 5 °C $min^{-1}$ and then to 240 °C at a rate of 20 °C $min^{-1}$, where it was left for 5 min. The temperatures of the injector source and mass spectrometer sources were set at 250 °C and 200 °C, respectively. The 30% terpinen-4-ol, 10-28% γ-terpinene, 5-13% α-terpinene, less than 15% 1,8-cineole, less than 12% p-cymene, 1,5-8% α-terpineol and small quantities of pinene, terpinolene, limonene, aromadendrene injection volume was 1 µl with a split ratio of 10:1. The constituent compounds of TTO were identified based on their mass spectra using mass spectra from the NIST 14 and Wiley 09 library.

## RESULTS AND DISCUSSIONS

The recorded chromatograms for the essential oils, and the chemical composition are presented in Figure 1, and Table 1, respectively. 23 compounds were identified in the TTO, with 8 compounds being present in all the analysed samples.

The main component was terpinen-4-ol (31.40-61.09%), followed by different compounds: 4.20-23.42% $\gamma$-terpinene, 0.48-10.05% $\alpha$-terpinene, 1.67-7.96 1,8-cineole, 3.16-9.49% *p*-cymene, 2.42-8.68% $\alpha$-terpineol and small quantities of $\alpha$-pinene (0.32-8.22%), $\alpha$-terpinolene (0.65-4.18%), limonene (1.07-9.14%), aromadendrene (n.d.-1.69%). The values of the concentration found in the present study for the major compounds are in the domain found in other studies that determined

the chemical composition on more than ninety five TTO samples: terpinen-4-ol (6.2–44.9%), terpinolene (0.04–45.7%), *γ*-terpinene (3.1–23.0%), *p*-cymene (0.3–19.4%), *cis*-sabinene hydrate (trace–19.4%), 1,8-cineole (0.5–18.3%), *α*-terpinene (2.3–11.7%), *α*-pinene (1.8–9.2%), *β*-phellandrene (trace–5.2%), and *α*-terpineol (1.9–4.2%) (de Groot and Schmidt, 2016), except for sample S5 that revealed a 61.09% terpinen-4-ol (Table 1.)

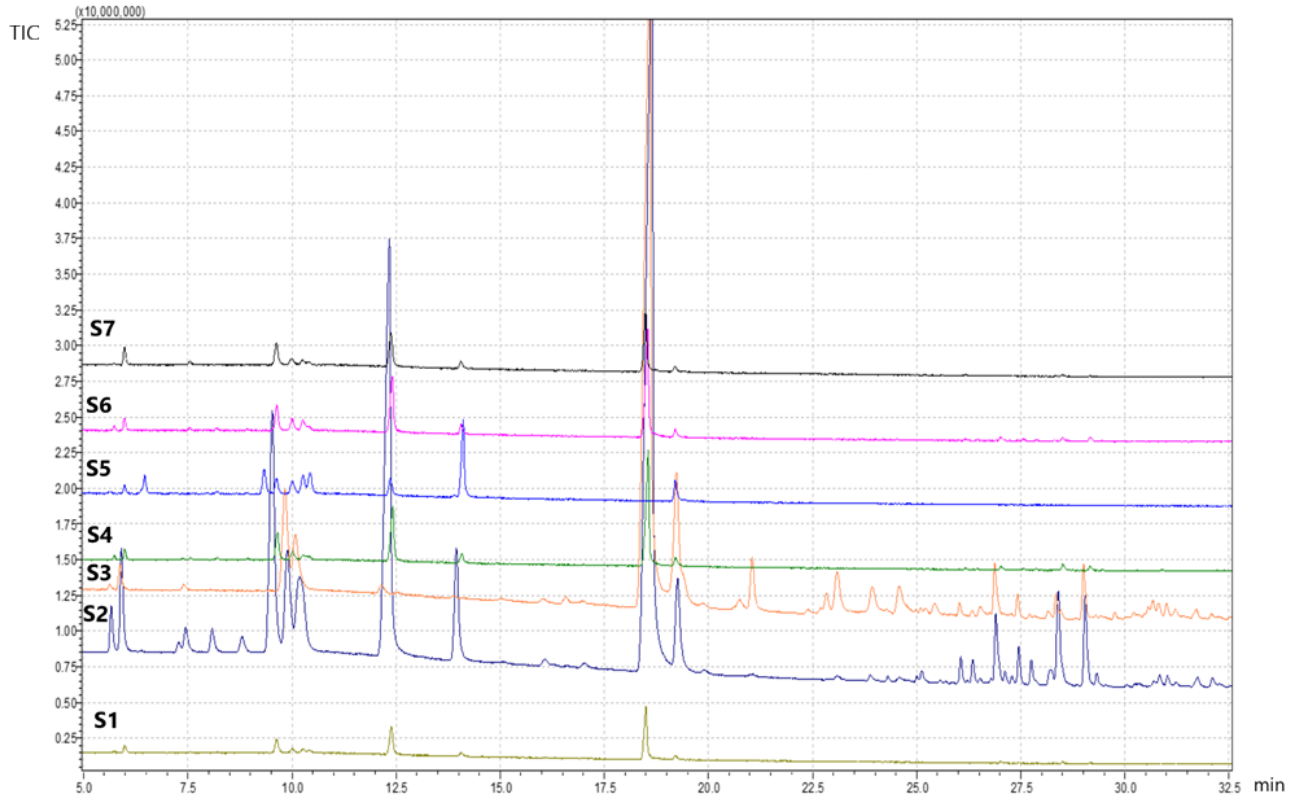


**Figure 1.** Overlapped chromatograms of *Tea tree* essential oils recorded for the analysed samples: S1-lime green; S2-indigo; S3-orange; S4-green; S5-blue; S6-pink; S7-black

The total percentage of terpenes was found to be from 20.94% in S5 to 56.67% in S1, while the total percentage of alcohols was found to be from 42.36% in S1 to 73.37% in S5. The total percentage of sesquiterpenes was found to be from 0.00% in S3 to 9.54% in S6 (Table 1).

**Table 1.** The chemical composition determined for the *Tea tree* essential oils analysed in this study.

| Compound | Chemical formula | Type of compound | RT (min) | Concentration (%) | | | | | | |
|---|---|---|---|---|---|---|---|---|---|---|
| | | | | **S1** | **S2** | **S3** | **S4** | **S5** | **S6** | **S7** |
| *α*-Thujene | $C_{10}H_{16}$ | T | 5.73 | n.d. | 1.05±0.06 | 0.55±0.15 | 1.16±0.21 | 0.15±0.01 | 1.07±0.01 | 0.65±0.18 |
| *α*-Pinene | $C_{10}H_{16}$ | T | 5.98 | 8.22±0.51 | 2.95±0.15 | 2.88±0.68 | 3.32±0.86 | 0.32±0.00 | 2.58±0.03 | 4.01±0.25 |
| Sabinene | $C_{10}H_{16}$ | T | 7.45 | n.d. | n.d. | 7.59±0.78 | 0.46±0.13 | n.d. | 0.23±0.03 | n.d. |
| *β*-Pinene | $C_{10}H_{16}$ | T | 7.56 | 1.57±0.01 | 0.61±0.11 | 0.38±0.56 | 0.54±0.24 | n.d. | 0.69±0.04 | n.d. |
| *β*-Myrcene | $C_{10}H_{16}$ | T | 8.19 | n.d. | 0.66±0.11 | 0.56±0.13 | 0.65±0.02 | n.d. | n.d. | n.d. |
| *α*-Phellandrene | $C_{10}H_{16}$ | T | 8.93 | n.d. | 0.39±0.12 | 11.07±0.36 | 0.44±0.10 | n.d. | 0.72±0.01 | n.d. |
| *α*-Terpinene | $C_{10}H_{16}$ | T | 9.63 | 14.65±0.58 | 9.34±0.38 | 6.10±0.66 | 10.05±0.50 | 5.59±0.02 | 0.48±0.04 | 10.89±0.25 |
| *p*-Cymene | $C_{10}H_{14}$ | T | 10.00 | 4.28±0.06 | 4.32±0.33 | 6.22±0.27 | 3.42±0.12 | 8.19±0.31 | 9.77±0.15 | 3.16±0.31 |
| 1,8-Cineol | $C_{10}H_{18}O$ | A | 10.27 | 2.68±0.16 | 4.10±0.37 | 7.96±0.81 | 1.67±0.03 | 4.36±0.01 | 3.80±0.05 | 2.45±0.30 |
| (+)-Limonene | $C_{10}H_{16}$ | T | 10.38 | 1.86±0.51 | 1.07±0.29 | 9.14±0.25 | 1.63±0.60 | 1.67±0.00 | 4.79±0.13 | 2.61±0.69 |
| *γ*-Terpinene | $C_{10}H_{16}$ | T | 12.38 | 21.92±0.69 | 21.88±0.39 | 6.85±0.35 | 21.56±0.60 | 4.20±0.02 | 18.89±0.04 | 23.42±1.45 |
| *α*-Terpinolene | $C_{10}H_{16}$ | T | 14.06 | 4.18±0.21 | 3.03±0.23 | 0.65±0.32 | 3.07±0.24 | 0.82±0.01 | 3.72±0.13 | 2.70±0.47 |
| **Terpinen-4-ol** | $C_{10}H_{18}O$ | A | 18.49 | **36.65±0.27** | **43.27±1.83** | **31.40±0.08** | **44.34±1.85** | **61.09±0.12** | **39.80±0.02** | **43.70±2.64** |
| *α*-Terpineol | $C_{10}H_{18}O$ | A | 19.20 | 3.03±0.14 | 2.42±0.23 | 8.68±0.30 | 2.78±0.09 | 7.92±0.01 | 3.75±0.27 | 3.18±0.15 |
| *α*-Gurjunene | $C_{15}H_{24}$ | ST | 26.17 | n.d. | 0.29±0.06 | n.d. | 0.20±0.05 | 0.45±0.01 | 0.54±0.01 | n.d. |
| Caryophyllene | $C_{15}H_{24}$ | ST | 26.46 | n.d. | 0.26±0.01 | n.d. | 0.19±0.13 | 0.20±0.02 | 0.46±0.10 | n.d. |
| Aromadendrene | $C_{15}H_{24}$ | ST | 27.01 | n.d. | 1.16±0.18 | n.d. | 0.90±0.20 | 2.11±0.01 | 1.68±0.12 | 1.69±0.08 |
| Longipinene | $C_{15}H_{24}$ | ST | 27.56 | n.d. | 0.41±0.01 | n.d. | 0.36±0.12 | n.d. | 0.78±0.12 | n.d. |
| Isoledene | $C_{15}H_{24}$ | ST | 27.86 | n.d. | 0.34±0.12 | n.d. | 0.29±021 | 0.80±0.00 | 0.57±0.04 | n.d. |
| Ledene | $C_{15}H_{24}$ | ST | 28.47 | 0.97±0.16 | 1.08±0.13 | n.d. | 1.88±0.26 | 2.13±0.01 | 2.95±0.29 | 0.93±0.43 |
| *δ*-Cadinene | $C_{15}H_{24}$ | ST | 29.16 | n.d. | 1.44±0.01 | n.d. | 1.15±0.00 | 5.59±0.01 | 2.33±0.01 | 0.64±0.40 |
| Cubenene | $C_{15}H_{24}$ | ST | 29.32 | n.d. | n.d. | n.d. | n.d. | n.d. | 0.25±0.01 | n.d. |
| Globulol | $C_{15}H_{26}O$ | A | 30.84 | n.d. | n.d. | n.d. | n.d. | n.d. | 0.20±0.01 | n.d. |
| | Total | T | | 56.67 | 45.27 | 51.97 | 46.27 | 20.94 | 42.92 | 47.43 |
| | | A | | 42.36 | 49.78 | 48.03 | 48.79 | 73.37 | 47.54 | 49.32 |
| | | ST | | 0.97 | 4.96 | 0.00 | 4.95 | 5.69 | 9.54 | 3.26 |

n. d. : not determined; T: terpene; ST: sesquiterpene; A: alcohol. The values are expressed in mean ±standard deviation.

## CONCLUSIONS

The determination of the chemical composition of tea tree essential oil (TTO) available on the market was carried out using a gas chromatograph apparatus equipped with a mass spectrometer as a detector. We carried out this study as our initial hypothesis was that the identification of the TTO chemotype and the minor compounds found in different products from the market is important and probably could be displayed on the product label more widely, to help the consumer in choosing the most suitable product for personal use, to minimize the occurrence of allergic reactions as side effects. It was shown that all the TTO samples investigated showed a terpinen-4-ol chemotype, the compound found in the highest concentration.

## ACKNOWLEDGMENTS

We thank Prof. Ülo Niinemets from Estonian University of Life Sciences, Tartu, Estonia, for his generous gift (one TTO sample).

## REFERENCES

Amarowicz, R., Pegg, R.B., 2019. Natural antioxidants of plant origin, in: Ferreira, I., Barros, L. (Eds.), Functional Food Ingredients from Plants, pp 1-81.

Amer, S.S., Nasr, M., Abdel-Aziz, R.T.A., Moftah, N.H., El Shaer, A., Polycarpou, E., Mamdouh, W., Sammour, O., 2020. Cosm-nutraceutical nanovesicles for acne treatment: Physicochemical characterization and exploratory clinical experimentation. International Journal of Pharmaceutics 577.

Avonto, C., Chittiboyina, A.G., Wang, M., Vasquez, Y., Rua, D., Khan, I.A., 2016. In Chemico Evaluation of Tea Tree Essential Oils as Skin Sensitizers: Impact of the Chemical Composition on Aging and Generation of Reactive Species. Chemical Research in Toxicology 29, 1108-1117.

Bedini, S., Cosci, F., Tani, C., Pierattini, E.C., Venturi, F., Lucchi, A., Ioriatti, C., Ascrizzi, R., Flamini, G., Ferroni, G., Taglieri, I., Conti, B., 2020. Essential Oils as Post-Harvest Crop Protectants against the Fruit FlyDrosophila suzukii: Bioactivity and Organoleptic Profile. Insects 11.

Borotova, P., Galovicova, L., Vukovic, N.L., Vukic, M., Tvrda, E., Kacaniova, M., 2022. Chemical and Biological Characterization of Melaleuca alternifolia Essential Oil. Plants-Basel 11.

Braun, L., 2007. Tea-tree. Journal of Complementary Medicine 6, 64-66.

Brun, P., Bernabe, G., Filippini, R., Piovan, A., 2019. In Vitro Antimicrobial Activities of Commercially Available Tea Tree (Melaleuca alternifolia) Essential Oils. Current Microbiology 76, 108-116.

Carson, C.F., Ashton, L., Dry, L., Smith, D.W., Riley, T.V., 2001. Melaleuca alternifolia (tea tree) oil gel (6%) for the treatment of recurrent herpes labialis. Journal of Antimicrobial Chemotherapy 48, 450-451.

Carson, C.F., Hammer, K.A., Riley, T.V., 2006. Melaleuca alternifolia (Tea Tree) oil: a review of antimicrobial and other medicinal properties. Clinical microbiology reviews 19, 50-62.

Carson, C.F., Smith, D.W., Lampacher, G.J., Riley, T.V., 2008. Use of deception to achieve double-blinding in a clinical trial of Melaleuca alternifolia (tea tree) oil for the treatment of recurrent herpes labialis. Contemporary Clinical Trials 29, 9-12.

Cox, S.D., Mann, C.M., Markham, J.L., Gustafson, J.E., Warmington, J.R., Wyllie, S.G., 2001. Determining the Antimicrobial Actions of Tea Tree Oil. Molecules : A Journal of Synthetic Chemistry and Natural Product Chemistry 6, 87-91.

da Silva, R.A., Antonieti, F., Roder, D.V.D., Pedroso, R.D., 2021. Essential Oils of Melaleuca, Citrus, Cupressus, and Litsea for the Management of Infections Caused by Candida Species: A Systematic Review. Pharmaceutics 13.

de Figueiredo, M., 2006. Chemical composition and oil concentration of tea tree leaf oil grown in South Africa during a one-year vegetative cycle. Journal of Essential Oil Research 18, 52-53.

de Groot, A.C., Schmidt, E., 2016. Tea tree oil: contact allergy and chemical composition. Contact Dermatitis 75, 129-143.

Edris, A.E., 2007. Pharmaceutical and therapeutic Potentials of essential oils and their

individual volatile constituents: a review. Phytotherapy Research 21, 308-323.

Gao, Y.-Y., Xu, D.-l., Huang, l.-J., Wang, R., Tseng, S.C.G., 2012. Treatment of Ocular Itching Associated With Ocular Demodicosis by 5% Tea Tree Oil Ointment. Cornea 31.

Hartford, O., Zug, K.A., 2005. Tea tree oil. Cutis 76, 178-180.

Jammy, R., Japar, S., Shah, M.K.M., 2015. Physicochemical and Mechanical Properties of Different Morphological Parts of the Tea Tree (Melaleuca alternifolia) Fibres. Fibres & Textiles in Eastern Europe 23, 31-36.

Lee, L.S., Brooks, L.O., Homer, L.E., Rossetto, M., Henry, R.J., Baverstock, P.R., 2002. Geographic variation in the essential oils and morphology of natural populations of Melaleuca alternifolia (Myrtaceae). Biochemical Systematics and Ecology 30, 343-360.

Melo, A.D.B., Amaral, A.F., Schaefer, G., Luciano, F.B., de Andrade, C., Costa, L.B., Rostagno, M.H., 2015. Antimicrobial effect against different bacterial strains and bacterial adaptation to essential oils used as feed additives. Canadian Journal of Veterinary Research-Revue Canadienne De Recherche Veterinaire 79, 285-289.

Nikolic, M.M., Jovanovic, K.K., Markovic, T.L., Markovic, D.L., Gligorijevic, N.N., Radulovic, S.S., Kostic, M., Glamoclija, J.M., Sokovic, M.D., 2017. Antimicrobial synergism and cytotoxic properties of Citrus limon L., Piper nigrum L. and Melaleuca alternifolia (Maiden and Betche) Cheel essential oils. Journal of Pharmacy and Pharmacology 69, 1606-1614.

Noumi, E., Snoussi, M., Hajlaoui, H., Trabelsi, N., Ksouri, R., Valentin, E., Bakhrouf, A., 2011. Chemical composition, antioxidant and antifungal potential of Melaleuca alternifolia (tea tree) and Eucalyptus globulus essential oils against oral Candida species. Journal of Medicinal Plants Research 5, 4147-4156.

Padalia, R.C., Verma, R.S., Chauhan, A., Goswami, P., Verma, S.K., Darokar, M.P., 2015. Chemical composition of Melaleuca linarrifolia Sm. from India: a potential source of 1,8-cineole. Industrial Crops and Products 63, 264-268.

Palmeira-De-Oliveira, A., Salgueiro, L., Palmeira-De-Oliveira, R., Martinez-De-Oliveira, J., Pina-Vaz, C., Queiroz, J.A., Rodrigues, A.G., 2009. Anti-Candida Activity of Essential Oils. Mini-Reviews in Medicinal Chemistry 9, 1292-1305.

Pauli, A., Schilcher, H., 2016. In Vitro Antimicrobial Activities of Essential Oils Monographed in the European Pharmacopoeia 8th Edition.

Santos, R.C.V., Soares Lopes, L.Q., Alves, C.F.D., Fausto, V.P., Pizzutt, K., Barboza, V., De Souza, M.E., Raffin, R.P., Gomes, P., Takamatsu, D., Morinaga, Y., Boligon, A.A., Athayde, M.L., Felippi, C.C., Vaucher, R.D.A., 2014. Antimicrobial activity of tea tree oil nanoparticles against American and European foulbrood diseases agents. Journal of Asia-Pacific Entomology 17, 343-347.

Setzer, W.N., Vogler, B., Schmidt, J.M., Leahy, J.G., Rives, R., 2004. Antimicrobial activity of Artemisia douglasiana leaf essential oil. Fitoterapia 75, 192-200.

Sevik, R., Akarca, G., Kilinc, M., Ascioglu, C., 2021. Chemical Composition of Tea Tree (Melaleuca alternifolia) (Maiden & Betche) Cheel Essential Oil and Its Antifungal Effect on Foodborne Molds Isolated from Meat Products. Journal of Essential Oil Bearing Plants 24, 561-570.

Sgorbini, B., Cagliero, C., Argenziano, M., Cavalli, R., Bicchi, C., Rubiolo, P., 2017. In vitro release and permeation kinetics of Melaleuca alternifolia (tea tree) essential oil bioactive compounds from topical formulations. Flavour and Fragrance Journal 32, 354-361.

Sharifi-Rad, J., Salehi, B., Varoni, E.M., Sharopov, F., Yousaf, Z., Ayatollahi, S.A., Kobarfard, F., Sharifi-Rad, M., Afdjei, M.H., Sharifi-Rad, M., Iriti, M., 2017. Plants of the Melaleuca Genus as Antimicrobial Agents: From Farm to Pharmacy. Phytotherapy Research 31, 1475-1494.

Yadav, E., Kumar, S., Mahant, S., Khatkar, S., Rao, R., 2017. Tea tree oil: a promising essential oil. Journal of Essential Oil Research 29, 201-213.

Yong, Y., Fang, B., Huang, Y., Li, J., Yu, T., Wu, L., Hu, C., Liu, X., Yu, Z., Ma, X., Gooneratne, R., Li, S., Abd El-Aty, A.M., Ju,

X., 2022. Tea Tree Oil Terpinen-4-ol Protects Gut Barrier Integrity by Upregulation of Tight Junction Proteins via the ERK1/2-Signaling Pathway. Frontiers in Nutrition 8.

ISSN 1582-1021
e-ISSN 2668-4764
Edited by "AUREL VLAICU" University
Arad, Romania



10.62591/Scien.Tech.Bull-Chem.FoodSci.Eng.2021.18.04

*ARTICLE*

# GREEN SYNTHESIS AND CHARACTERIZATION OF SILVER NANOPARTICLES OBTAINED FROM *THYMUS VULGARIS* L. HYDROLAT

**Alina CIUREL[1], Andreea LUPITU[2], Lucian COPOLOVICI[2], Cristian MOISA[2*], Dana COPOLOVICI[2]**

*[1]Biomedical Sciences Doctoral School, University of Oradea, 1 University St., 410087 Oradea, Romania*
*[2]Faculty of Food Engineering, Tourism and Environmental Protection, Institute for Research, Development and Innovation in Technical and Natural Sciences, Aurel Vlaicu University, Elena Drăgoi St. No. 2, 310330 Arad, Romania*
*Corresponding author email: moisa.cristian@yahoo.com*

***Abstract:*** *The essential oil industry has grown over the last decade and is generating a lot of useful by-products with diverse industrial applications in food, cosmetics, textile, and more recently in phytosynthesis of metal nanoparticles. GC-MS analysis performed on the hydrolat identified 18 out of the 21 compounds detected, and the major terpenic class was represented by oxygenated monoterpenes 92.63% (1-octen-3-ol, endo-borneol, carvacrol methyl ether, thymol, carvacrol). Obtaining quasi-spherical silver nanoparticles from hydrolat and 0.1 mM $AgNO_3$ solution was simple, effective, and non-toxic, yielding stable nanoparticles with average particle size under 45 nm. UV-Vis spectroscopy revealed a strong signal at 438 nm indicating the formation of silver nanoparticles and SEM-EDX analysis revealed that elemental Ag was detected and confirmed by a strong signal at 3 keV with more than 91% silver.*

**Keywords**: bioactive compounds, by-products, green synthesis, hydrolat, silver nanoparticles.

## INTRODUCTION

Throughout the years the preference for green synthesis of metal nanoparticles (Maťátková et al., 2022) (mNPs) like silver (AgNPs), gold (AuNPs), platinum (PtNPs), and copper (CuNPs), has been observed (Kumar et al., 2021). Therefore, the continuous demand of mNPs in several fields of applications like biotechnology, engineering, functional textiles, electronics, environmental engineering, pharmaceuticals, water, and wastewater treatments (Hitesh and Lata, 2018) has focused the attention on phytosynthesis from plant-based extracts and by-products as reducing and capping agents (Popa et al., 2021; Vilas et al., 2014).

One representative medicinal plant belonging to the *Lamiaceae* family is the perennial subshrub *Thymus vulgaris* L. frequently found in the southern part of Europe like the Mediterranean region but with a worldwide distribution (Nasrollahzadeh et al., 2016). It is harvested and processed for its valuable essential oil is rich in oxygenated and hydrocarbonated monoterpenes (*p*-cymene, $\gamma$-terpinene, linalool, thymol, and carvacrol), alongside its phenolic compounds and flavonoids (Popa et al., 2021).

During the distillation process of medicinal and aromatic plants, the essential oils are carried out by the water vapours and while passing through the condenser, a mixture of water and essential oil is collected. After the separation, two phases are obtained, namely essential oil and hydrolat (Stahl-Biskup and Saez, 2003). While essential oils represent complex mixtures of monoterpenes and sesquiterpenes, their corresponding hydrolats are composed of 99% water (Labadie et al., 2015; Šilha et al., 2020).

The slightly more water-soluble terpenes impregnate the hydrolat with its specific scent (Martínez-Gil et al., 2013; Smail et al., 2011) providing them with the potential of metal salts reduction in green NPs synthesis. Industrially, hydrolats are considered invaluable by-products and are discarded (Garzoli et al., 2020; Martínez-Gil et al., 2013), or have food and cosmetic applications (Paolini et al., 2008).

Taking into consideration that medicinal and aromatic plants are intensively used to this day for their bioactive compounds (Moisă et al., 2018; Moisa et al., 2019), understanding and using by-products (hydrolats) (Popa et al., 2021) resulted from the essential oil (EO) industry as reducing and capping agents for metal

nanoparticles synthesis is a promising alternative to classical synthesis.

Therefore, the present study aimed to use *Thymus vulgaris* hydrolats containing traces of dissolved essential oils, as mediators for the green synthesis of silver nanoparticles. To our knowledge, AgNPs from thyme hydrolats has not been obtained.

## MATERIALS AND METHODS

All utilized chemicals and reagents were of suitable analytical grade purchased from Sigma-Aldrich and Merck.

*Plant material and source*

Fresh herbs of *Thymus vulgaris* L. were obtained from a local producer in Arad County. After harvesting, the plant material was airdried and stored in paper bags until needed.

*EO and hydrolat extraction*

Dried thyme plants were steam-distilled and the water–essential oil mixture was separated by density.

*Hydrolat volatile compounds extraction*

The resulting hydrolat was prepared for analysis after a liquid-liquid extraction step as follows: 1 mL hexane and 25 mL hydrolat kept in an ultrasound bath for 1 hour using the Elmasonic TI-H5 (Elma, Schimdbauer GmbH, Germany). After sonication, the mixture was separated using a Hettich ultracentrifuge (Rotina 380 R, Hettich GmbH, Tuttlingen, Germany) and the hexane layer was prepared for GC-MS analysis.

*Chemical composition determined by GC-MS analysis*

The resulting extract was analyzed by gas chromatography (GC, Shimadzu 2010, Kyoto, Japan) coupled with a mass spectrometer (MS, TQ 8040, Shimadzu, Kyoto, Japan). The GC-MS analysis method is described by (Chambre et al., 2020; Moisa et al., 2019).

*Extracts preparation for Ag-NPs synthesis*

The hydrolat was used immediately alongside 0.1 mM $AgNO_3$ solution with pH 8. Therefore, to 30 mL of boiling 0.1 mM $AgNO_3$ solution, 2 mL of hydrolat were added dropwise and mixed vigorously for 10 minutes on a hotplate magnetic stirrer. The reaction mixture was then transferred to another magnetic stirrer for 20 minutes without heat, to allow it to reach room temperature. The formation of AgNPs was confirmed visually by the colour change from a clear pale-yellow to a reddish-yellow or brown mixture.

*UV-Vis analysis*

The bio-reduction of $AgNO_3$ was monitored by scanning in the range of λ=300-800 nm using a UV-Vis spectrophotometer (Specord 200, Analytik Jena AG, Jena, Germany).

*SEM-EDX analysis of AgNPs*

To determine the morphology and size distribution of the obtained AgNPs, a scanning electron microscope was used (SEM, LYRA 3 XMU, Tescan, Czech Republic) coupled with an EDX - Energy Dispersive X-ray spectroscopy for elemental analysis (EDAX Inc., Mahwah, NJ, USA).

## RESULTS AND DISCUSSIONS

Taking into consideration that hydro distillation is still the most intensively used method for obtaining essential oils, a large amount of hydrolat is generated in the process.

The hydrolat chemical composition is strongly related to that of the essential oil, and the main factor influencing the distribution of terpenic compounds in hydrolat is their polarity (Labadie et al., 2015; Popa et al., 2021). Thus, because the main compounds in thyme essential oil are phenolic based, its corresponding hydrolat has a high amount of dissolved volatiles and its potential for green nanoparticles synthesis is higher (Popa et al., 2021).

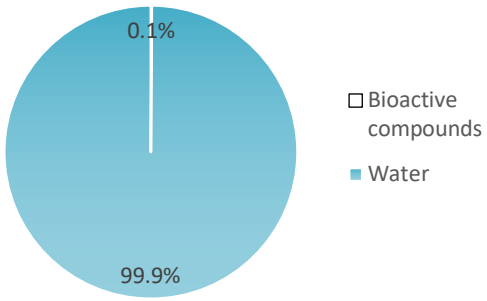


**Figure 1.** The average amount of bioactive compounds found in HD (Labadie et al., 2015)

*Hydrolat chemical composition*

After GC-MS analysis, 21 compounds were detected from which 18 were identified by comparing them with standards and by using the spectra libraries NIST 14, and Wiley 09.

The chemical composition of *Thymus vulgaris* hydrolat was composed mainly of oxygenated monoterpenes 92.63% (1-octen-3-ol, endo-borneol, carvacrol methyl ether, thymol, carvacrol). Hydrocarbonated monoterpenes and sesquiterpenes accounted only for 5.16%, and 2.2% of the compounds weren't identified.

As reported by other studies (Labadie et al., 2015; Popa et al., 2021) oxygenated compounds have a higher water solubility, therefore in thyme hydrolat the total amount of dissolved volatiles is higher making it suitable for Ag NPs synthesis.

**Table 1.** *Thymus vulgaris* hydrolat chemical composition

| Nr. Crt. | RI | Compound name | Amount (%) |
|---|---|---|---|
| 1 | 930 | *α*-Thujene | 0.07 |
| 2 | | ND | 1.57 |
| 3 | 977 | 1-Octen-3-ol | 1.7 |
| 4 | 980 | 3-Octanol | 0.84 |
| 5 | 1024 | *p*-cymene | 2.33 |
| 6 | 1059 | *γ*-terpinene | 0.12 |
| 7 | 1070 | *cis*-Sabinene hydrate | 0.64 |
| 8 | 1096 | Linalool | 0.67 |
| 9 | 1169 | endo-Borneol | 1.76 |
| 10 | 1235 | Thymol methyl ether | 0.57 |
| 11 | 1244 | Carvacrol methyl ether | 1.68 |
| 12 | 1287 | Bornyl acetate | 0.22 |
| 13 | 1290 | Thymol | 63.77 |
| 14 | 1299 | Carvacrol * | 21.42 |
| 15 | 1376 | *α*-Copaene | 0.08 |
| 16 | 1419 | *β*-Caryophyllene * | 0.67 |
| 17 | 1441 | Aromandrene | 0.93 |
| 18 | 1481 | Germacrene D | 0.32 |
| 19 | | ND | 0.56 |
| 20 | 1583 | Caryophyllene oxide | 0.01 |
| 21 | | ND | 0.07 |

The RI was calculated compared to n-alkanes (C10 to C35) and the compounds marked with an asterisk (*) were identified using analytical standards.

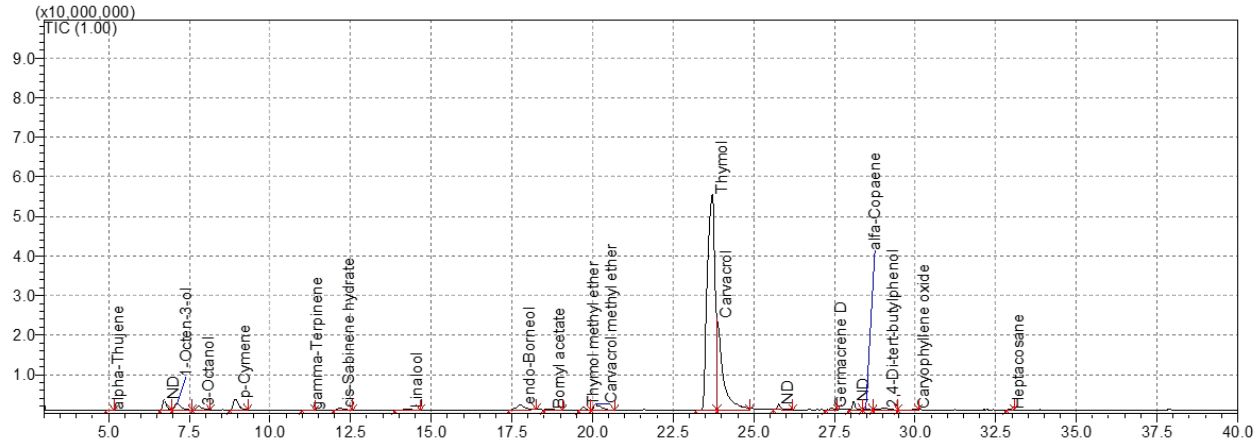


**Figure 2.** *Thymus vulgaris* hidrolat chromatorgram

*UV-Vis Ag-NPs analysis*

The bio-reduction of silver ions was mediated by the dissolved phenolic compounds present in the thyme hydrolat. This process was easily observed in the resulted reaction mixture by a visual colour change and confirmed by UV-Vis spectral analysis and a high value was recorded at 438 nm, specific for AgNPs with an average particle size of around 50-70 nm (Agnihotri et al., 2014).

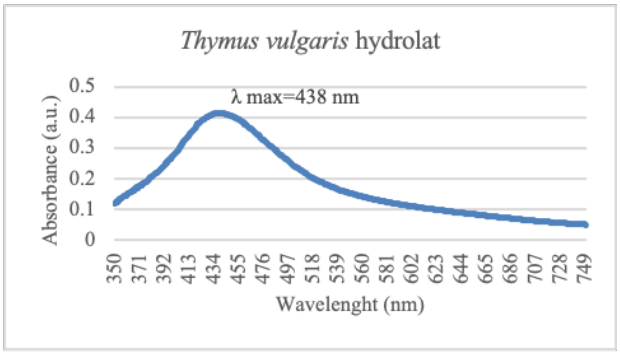


**Figure 3.** UV-Vis spectra of hydrolat biosynthesized AgNPs

*SEM-EDX analysis of AgNPs*

To analyse the particle size and surface morphology the obtained AgNPs mixture was centrifuged for 30 minutes at 10.000 rpm using a Hettich Rotina 380 R centrifuge and the AgNPs pellet was washed 3 times with ultrapure water. The purified AgNPs were placed on carbon tape, airdried and micrographs were recorded using a SEM at around 50kx magnification as presented in Figure 4.

The average particles shape was quasi-spherical and the size distribution was under 50 nm as presented in Table 2.

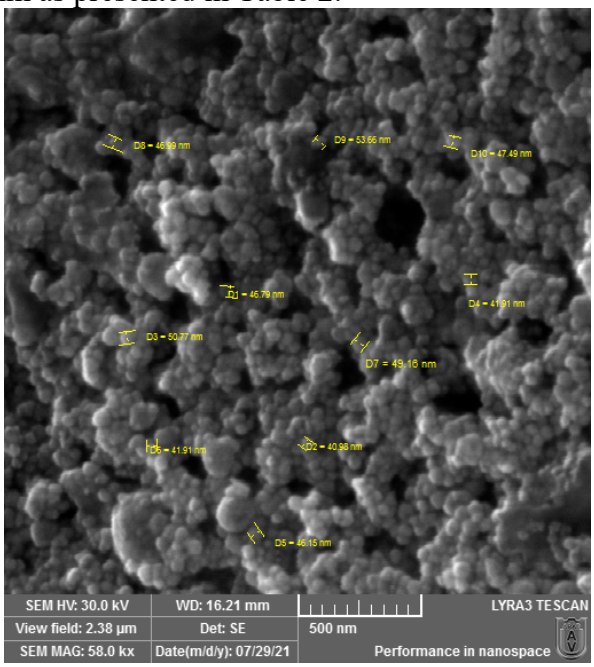


**Figure 4.** SEM micrograph of the hydrolat biosynthesized AgNPs

**Table 2.** Average size distribution of hydrolat biosynthesized AgNPs

| Value | **Hydrolat** |
|---|---|
| | d [nm] |
| Obj. count | 10 |
| Summation | 434.17 |
| Min. value | 36.28 |
| Max. value | 55.16 |
| Mean value | 43.42 |
| Std. dev. | 6.22 |

For further insight, the chemical composition of the resulted AgNPs was analysed by EDX, and elemental Ag was determined and confirmed by a strong signal at 3 keV representing more than 91% silver and minor quantities of carbon.

Figure 5 presents the EDX spectrum of the resulted AgNPs where no impurity peaks were detected. The EDX spectrum reveals the high purity of the resulted AgNPs.

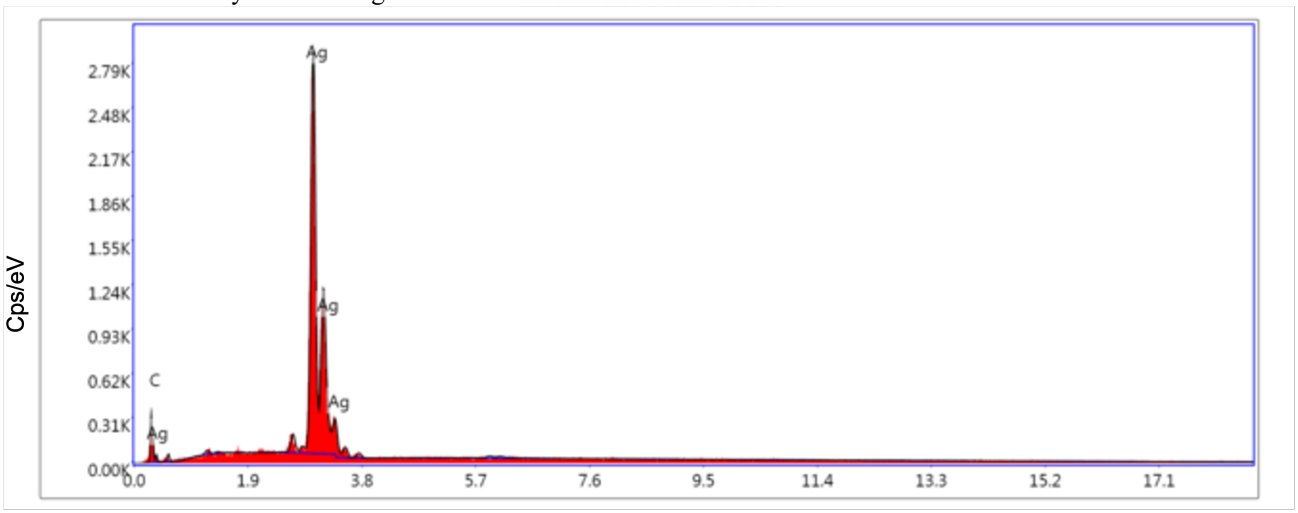


**Figure 5.** EDX spectrum of the hydrolat biosynthesized AgNP

## CONCLUSIONS

The dissolved biomolecules present in the *Thymus vulgaris* hydrolat, are safe to handle and have mediated stable and eco-friendly quasi-spherical AgNPs with small average particle size.

SEM-EDX analysis confirmed the reduction of $Ag^+$ to $Ag^0$ with an average particle size of 43 nm and over 91% silver content.

Using plant extracts has many benefits from accessibility to a wide range of secondary metabolites useful for obtaining benign metal NPs with no side effects.

## ACKNOWLEDGEMENTS

This work was supported by a grant from the Romanian Ministry of Education and Research, CNCS—UEFISCDI, project number PN-III-P1-1.1-PD-2019-0607, within PNCDI III.

## REFERENCES

Agnihotri, S., Mukherji, S., Mukherji, S., 2014. Size-controlled silver nanoparticles synthesized over the range 5–100 nm using the same protocol and their antibacterial efficacy. Rsc Advances 4, 3974-3983.

Chambre, D.R., Moisa, C., Lupitu, A., Copolovici, L., Pop, G., Copolovici, D.M., 2020. Chemical composition, antioxidant capacity, and thermal behavior of *Satureja hortensis* essential oil. Sci. Rep. 10, 21322.

Garzoli, S., Petralito, S., Ovidi, E., Turchetti, G., Laghezza Masci, V., Tiezzi, A., Trilli, J., Cesa, S., Casadei, M.A., Giacomello, P., Paolicelli, P., 2020. Lavandula x intermedia essential oil and hydrolate: Evaluation of chemical composition and antibacterial activity before and after formulation in nanoemulsion. Industrial Crops and Products 145, 112068.

Hitesh, Lata, S., 2018. Green Chemistry Based Synthesis of Silver Nanoparticles from Floral Extract of Nelumbo Nucifera. Materials Today: Proceedings 5, 6227-6233.

Kumar, J.A., Krithiga, T., Manigandan, S., Sathish, S., Renita, A.A., Prakash, P., Prasad, B.S.N., Kumar, T.R.P., Rajasimman, M., Hosseini-Bandegharaei, A., Prabu, D., Crispin, S., 2021. A focus to green synthesis of metal/metal based oxide nanoparticles: Various mechanisms and applications towards ecological approach. Journal of Cleaner Production 324, 129198.

Labadie, C., Ginies, C., Guinebretiere, M.-H., Renard, C.M.G.C., Cerutti, C., Carlin, F., 2015. Hydrosols of orange blossom (*Citrus aurantium*), and rose flower (*Rosa damascena* and *Rosa centifolia*) support the growth of a heterogeneous spoilage microbiota. Int. Food Res. J. 76, 576-586.

Martínez-Gil, A.M., Pardo-García, A.I., Zalacain, A., Alonso, G.L., Salinas, M.R., 2013. Lavandin hydrolat applications to Petit Verdot vineyards and their impact on their wine aroma compounds. Int. Food Res. J. 53, 391-402.

Maťátková, O., Michailidu, J., Miškovská, A., Kolouchová, I., Masák, J., Čejková, A., 2022. Antimicrobial properties and applications of metal nanoparticles biosynthesized by green methods. Biotechnology Advances, 107905.

Moisă, C., Copolovici, L., Bungau, S., Pop, G., Imbrea, I., Lupitu, A.-I., Nemeth, S., Copolovici, D., 2018. Wastes resulting from aromatic plants distillation - bio-sources of antioxidants and phenolic compounds with biological active principles. Farmacia 66, 289-295.

Moisa, C., Lupitu, A., Pop, G., Chambre, D.R., Copolovici, L., Cioca, G., Bungau, S., Copolovici, D.M., 2019. Variation of the Chemical Composition of *Thymus Vulgaris* Essential Oils by Phenological Stages. Rev. Chim-Bucharest 70, 633-637.

Nasrollahzadeh, M., Sajadi, S.M., Rostami-Vartooni, A., Hussin, S.M., 2016. Green synthesis of CuO nanoparticles using aqueous extract of Thymus vulgaris L. leaves and their catalytic performance for N-arylation of indoles and amines. Journal of Colloid and Interface Science 466, 113-119.

Paolini, J., Leandri, C., Desjobert, J.-M., Barboni, T., Costa, J., 2008. Comparison of liquid–liquid extraction with headspace methods for the characterization of volatile fractions of commercial hydrolats from typically Mediterranean species. J. Chromatogr. A. 1193, 37-49.

Popa, C.L., Lupitu, A., Mot, M.D., Copolovici, L., Moisa, C., Copolovici, D.M., 2021. Chemical and Biochemical Characterization of Essential Oils and Their Corresponding Hydrolats from Six Species of the Lamiaceae Family. Plants 10, 2489.

Šilha, D., Švarcová, K., Bajer, T., Královec, K., Tesařová, E., Moučková, K., Pejchalová, M., Bajerová, P., 2020. Chemical Composition of Natural Hydrolates and Their Antimicrobial Activity on Arcobacter-Like Cells in Comparison with Other Microorganisms. Molecules 25.

Smail, A., Badiaa, L., Miguel, M., 2011. Antioxidant activity of some Morrocan hydrosols. J. Med. Plant Res.

Stahl-Biskup, E., Saez, F., 2003. Thyme: The Genus Thymus. CRC Press.
Vilas, V., Philip, D., Mathew, J., 2014. Catalytically and biologically active silver nanoparticles synthesized using essential oil. Spectrochimica Acta Part A: Molecular and Biomolecular Spectroscopy 132, 743-750.

ISSN 1582-1021
e-ISSN 2668-4764
Edited by "AUREL VLAICU" University
Arad, Romania



10.62591/Scien.Tech.Bull-Chem.FoodSci.Eng.2021.18.05

*ARTICLE*

# FATTY ACIDS PROFILE OF SOME COMMERCIALLY FISH ROE

**Carmen POPA [1], Iulia TIMOFTE [2], Lucian COPOLOVICI [2], Dana Maria COPOLOVICI [2*]**

*[1] University of Oradea, Biomedical Sciences Doctoral School, 1 University St., 410087, Oradea, Romania*

*[2] Aurel Vlaicu University, Faculty of Food Engineering, Tourism and Environmental Protection; Institute for Research, Development and Innovation in Technical and Natural Sciences, Romania, 2 Elena Dragoi St., Arad, 310330, Romania*

**Corresponding author: dana.copolovici@uav.ro*

***Abstract:*** *The demand for natural food sources and food ingredients is increasing, and fish roes are known to present high levels of ω-3 fatty acids (FA). In this work, we used gas-chromatography and UV spectroscopy (GC-DAD) to characterize the FA profile of six different commercial fish roes. The increase of concentration of ω-3 FA is tarama < hering < pike < cod < salmon < lumpfish. Altogether, the fish roes are an important source of unsaturated fatty acids (minimum 26.62% for pike roe) and present a modest source of saturated fatty acids (less than 46.45% for pike roe). Overall, this study provides a preliminary screening of FA profiles between several commercial fish roes.*

**Keywords**: fish roe, fatty acids, gas chromatography, mass spectrometry.

## Introduction

The beneficial effects of fish and fish oil consumption on human health are widely documented in the scientific literature (Abdelhamid et al., 2020; Abdelhamid et al., 2018; Alagawany et al., 2019; Cretton et al.). There have been many studies that have verified a reduction in the incidence of a variety of diseases, including cardiovascular disease (de la Guia-galipienso et al., 2021), cancer (de Castro et al., 2022; Franchi et al., 2022; Hsieh et al., 2022; Jiang et al., 2021; Laumann et al., 2022; Stasiewicz et al., 2022; Wang et al., 2022; Zhang et al., 2022), inflammatory (Dawczynski et al., 2018) and autoimmune disorders (AlAmmar et al., 2021; Lofvenborg et al., 2014), as well as psychiatric and mental ailments (Berger et al., 2017; Hansen et al., 2020; Sikka et al., 2021; Yonezawa et al., 2020). Fish liver oil, mushrooms, and other sources of vitamins are the best sources of vitamin D, besides exposure to the sun, for the average person. 1,25-dihydroxyvitamin D is primarily responsible for maintaining calcium and phosphorus balance in the body (de la Guia-galipienso et al., 2021). Many extra-skeletal effects of vitamin D, including those on the immune and cardiovascular (CV) systems, can be detected in human cells and tissues that contain vitamin D receptors. Blood pressure is regulated by vitamin D's effect on endothelium and smooth muscle cells. This vitamin deficiency has been linked to an increased risk of cardiovascular disease (CVD) death and incidence (de la Guia-galipienso et al., 2021).

Health advantages of a diet containing fish products are attributed to polyunsaturated fatty acids (PUFA), mainly omega-3 fatty acids; e.g., eicosapentaenoic acid: EPA and docosahexaenoic acid: DHA.

The fatty acids (FA) present in four lipid fractions [polar lipids (PL), diacylglycerols (DAG), free fatty acids (FFA), and triacylglycerols (TAG)] of common carp were investigated by Chvalova, D. and J. Spicka in (Chvalova and Spicka, 2016). There were differences across the examined tissues in terms of the amounts of lipid fractions and fatty acids that were classified as: saturated fatty acids (SFA), monounsaturated fatty acids (MUFA), polyunsaturated fatty acids (PUFA), and furan fatty acids (F-acids). Forty-nine compounds were identified in this research, from which eight F-acids were discovered in the tissues under investigation. In carp muscle, MUFA predominated because it accounted for nearly half of the total fatty acids: 51.8% in TAG, followed by SFA: 29.3% and PUFA: 19.0%. PUFA represented the majority of the PL 54.8%, followed by SFA: 26.6% and

MUFA: 18.5%, similar to that reported in [25]. Carp muscle tissue contained only negligible amounts of F-acids, less than 0.05%. The composition of PL in male and female gonad tissues was found to be comparable to that of muscle PL (a high amount of PUFA, followed by SFA and MUFA), which was previously observed.

It was discovered that the triacylglycerol fraction of male gonad tissue contained the highest concentration of F-acids. F-acids were found in polar lipids and diacylglycerols in female gonad tissue, albeit at a significantly lower concentration than in male gonad tissue (Chvalova and Spicka, 2016).

This study aimed to develop a method for determining the fatty acids in fish roe and screening the FA profile of some common commercial fish roe.

## MATERIALS AND METHODS

All the solvents (*n*-hexane, *n*-heptane, methanol, sulphuric acid) were of analytical grade and chromatographic purity (acetonitrile), respectively, acquired from Merck KGaA, Darmstadt, Germany.

Commercial fish roes (tamara, cod, herring, lumpfish, salmon, and pike) from the supermarket were bought and used in 2018. The lipid phase was extracted with *n*-hexane, and the supernatant was derivatized according to the method published by Copolovici et al., 2017, to obtain the corresponding fatty acid methyl esters (Copolovici et al., 2017). These esters were identified by using GC-MS (Shimadzu 2010, Tokyo, Japan), mass spectrometry data from commercial libraries (NIST and Wiley) as presented in (Copolovici et al., 2017), and overlapping chromatograms are depicted in Figure 1.

## RESULTS AND DISCUSSIONS

Prior studies have shown high amounts of PUFA in fish roe, with some articles reporting levels as high as 50% of total FA (Al-Sayed Mahmoud et al., 2008; Intarasirisawat et al., 2011). Docosahexaenoic acid (C22:6 n-3) was found to be the most abundant fatty acid (20.53–26.19%) in crude lipids extracted from tuna roes (51.22–54.90% of total lipids) (Al-Sayed Mahmoud et al., 2008). In our study, the values of PUFA are found to be from 26.61% in pike roe to 45.52% in cod roe (Table 1.)

In the present study, we found out that in the analyzed fish roes, the concentration of fatty acids varies depending on the species, so the myristic acid was found in a proportion of 3.55% in lumpfish roe and is increasing to up to 13.78% in pike roe. Elaidic acid was found in the samples analyzed, from 17.45% in pike roe to 26.26% in salmon roe (Figure 1).

As is revealed in Table 1, the fish roes analyzed present a good source of unsaturated fatty acids (UFA), with the following concentration for total ω-3 FA: tarama < herring < pike < cod < salmon < lumpfish, while ω-6 FA (linoleic acid) is found in a proportion of 6.46% in lumpfish roe and increase to 33.89% in tarama roe.

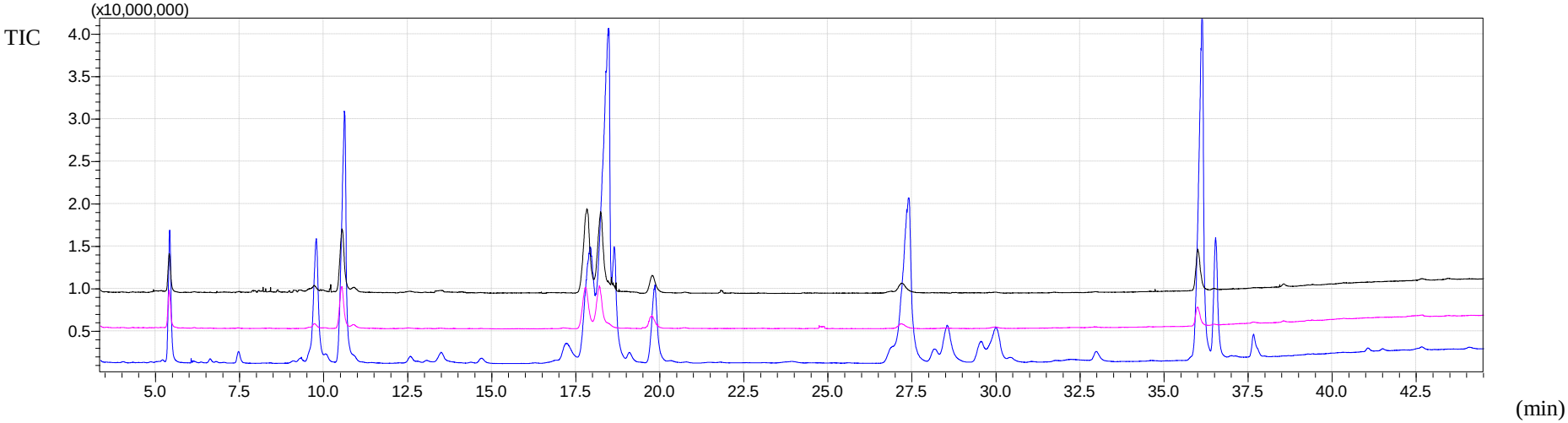


**Figure 1.** Overlapping chromatograms of salmon roe (blue), herring roe (pink), cod roe (black).

**Table 1**. Fatty acids identified in fish roe samples: the values are area expressed in % ($R_t$: retention time).

| **Fatty acid** | **Molecular formula** | **Molecular weight (Da)** | **$R_t$ (min)** | **Tarama roe** | **Cod roe** | **Hering roe** | **Lumpfish roe** | **Salmon roe** | **Pike roe** |
|---|---|---|---|---|---|---|---|---|---|
| Myristic acid (C14:0) | $C_{14}H_{28}O_2$ | 228.371 | 5,407 | 5.70±0.04 | 5.85±0.03 | 10.48±0.14 | 3.58±0.11 | 3.67±0.31 | 13.78±0.28 |
| Palmitoleic acid (C16:1, ω-7) | $C_{16}H_{30}O_2$ | 254.408 | 9,726 | 0.95±0.03 | 1.35±0.17 | 1.58±0.15 | 4.64±0.15 | 6.36±0.16 | 5.30±0.21 |
| Palmitic acid (C16:0) | $C_{16}H_{32}O_2$ | 256.424 | 10,552 | 16.48±0.17 | 16.30±0.42 | 19.65±0.21 | 13.62±0.02 | 11.45±0.14 | 22.50±0.35 |
| Linoleic acid (C18:2, ω-6) | $C_{18}H_{32}O_2$ | 280.445 | 17,844 | 33.89±0.12 | 31.89±0.12 | 26.84±0.08 | 6.46±0.15 | 9.42±0.13 | 14.16±0.21 |
| Elaidic acid(C18:1, ω-9) | $C_{18}H_{34}O_2$ | 282.461 | 18,251 | 23.34±0.48 | 20.73±0.04 | 19.73±0.04 | 24.34±0.18 | 26.26±0.20 | 17.45±0.21 |
| Oleic acid (C18:1, ω-7) | $C_{18}H_{34}O_2$ | 282.461 | 18,49 | 1.52±0.02 | 2.95±0.02 | 1.95±0.02 | 5.19±0.16 | 4.73±0.37 | 3.23±0.14 |
| Stearic acid (C18:0) | $C_{18}H_{36}O_2$ | 284.477 | 19,821 | 9.58±0.11 | 6.39±0.16 | 7.24±0.06 | 4.84±0.24 | 4.84±0.26 | 10.17±0.09 |
| Eicosapentanoic acid (C20:5, ω-3) | $C_{20}H_{30}O_2$ | 302.451 | 27,182 | 2.57±0.27 | 2.57±0.25 | 2.57±0.27 | 15.82±0.62 | 14.23±0.32 | 1.89±0.16 |
| Docosahexaenoic acid (C22:6, ω-3) | $C_{22}H_{32}O_2$ | 328.488 | 36,002 | 5.75±0.21 | 11.06±0.06 | 9.42±0.11 | 20.93±0.05 | 18.45±0.14 | 10.56±0.31 |
| Σ SFA | | | | 31.76 | 28.54 | 37.37 | 22.00 | 19.96 | 46.45 |
| Σ MUFA | | | | 25.81 | 25.02 | 23.245 | 34.16 | 37.34 | 25.98 |
| Σ PUFA | | | | 42.20 | 45.52 | 38.83 | 43.20 | 42.09 | 26.61 |
| Σ MUFA+ Σ PUFA | | | | 68.01 | 70.54 | 62.08 | 77.36 | 79.43 | 52.59 |
| Σ SFA/ Σ UFA | | | | 0.47 | 0.40 | 0.60 | 0.28 | 0.25 | 0.88 |
| Σ PUFA/ Σ MUFA | | | | 1.64 | 1.82 | 1.67 | 1.26 | 1.13 | 1.02 |

## CONCLUSIONS

Saturated fatty acids include palmitic acid (C16: 0) as the predominant FA in the analyzed samples, with a maximum of 22.5% in pike roe. The concentration of monounsaturated ω-7 fatty acids (palmitoleic acid and oleic acid) varied between 2.47% (tarama roe) and 11.08% (salmon roe), while for ω-9 fatty acid varied from 17.45% (pike roe) to 26.26% (salmon roe). Polyunsaturated fatty acids are smaller than 45.52%, while the concentration of ω-3 fatty acids varied from 8.32% in tarama roe to 36.74% in lumpfish roe. The PUFA / MUFA ratio varies between 1.02% for pike roe and 1.82% for cod roe. Further studies are required to quantify the fatty acids from commercial fish roes and determine their correlation between chemical composition and biological activities.

## ACKNOWLEDGEMENTS

Funding for the equipment used in the study has been provided by The European Commission and The Romanian Government (project POS CCE 621/2014).

## REFERENCES

Abdelhamid, A.S., Brown, T.J., Brainard, J.S., Biswas, P., Thorpe, G.C., Moore, H.J., Deane, K.H., Summerbell, C.D., Worthington, H.V., Song, F.J., Hooper, L., 2020. Omega-3 fatty acids for the primary and secondary prevention of cardiovascular disease. Cochrane Database of Systematic Reviews.

Abdelhamid, A.S., Brown, T.J., Brainard, J.S., Biswas, P., Thorpe, G.C., Moore, H.J., Deane, K.H.O., AlAbdulghafoor, F.K., Summerbell, C.D., Worthington, H.V., Song, F.J., Hooper, L., 2018. Omega-3 fatty acids for the primary and secondary prevention of cardiovascular disease. Cochrane Database of Systematic Reviews, CD003177.

Al-Sayed Mahmoud, K., Linder, M., Fanni, J., Parmentier, M., 2008. Characterisation of the lipid fractions obtained by proteolytic and chemical extractions from rainbow trout (Oncorhynchus mykiss) roe. Process Biochemistry 43, 376-383.

Alagawany, M., Elnesr, S.S., Farag, M.R., Abd El-Hack, M.E., Khafaga, A.F., Taha, A.E., Tiwari, R., Yatoo, M.I., Bhatt, P., Khurana, S.K., Dhama, K., 2019. Omega-3 and Omega-6 Fatty Acids in Poultry Nutrition: Effect on Production Performance and Health. Animals 9.

AlAmmar, W.A., Albeesh, F.H., Ibrahim, L.M., Algindan, Y.Y., Yamani, L.Z., Khattab, R.Y., 2021. Effect of omega-3 fatty acids and fish oil supplementation on multiple sclerosis: a systematic review. Nutritional Neuroscience 24, 569-579.

Berger, M.E., Smesny, S., Kim, S.W., Davey, C.G., Rice, S., Sarnyai, Z., Schlogelhofer, M., Schafer, M.R., Berk, M., McGorry, P.D., Amminger, G.P., 2017. Omega-6 to omega-3 polyunsaturated fatty acid ratio and subsequent mood disorders in young people with at-risk mental states: a 7-year longitudinal study. Translational Psychiatry 7.

Chvalova, D., Spicka, J., 2016. Identification of furan fatty acids in the lipids of common carp (Cyprinus carpio L.). Food Chemistry 200, 183-188.

Copolovici, D., Bungau, S., Boscencu, R., Tit, D.M., Copolovici, L., 2017. The Fatty Acids Composition and Antioxidant Activity of Walnut Cold Press Oil. Revista De Chimie 68, 507-509.

Cretton, M., Malanga, G., Sobczuk, T.M., Mazzuca, M., Marine lipids as a source of high-quality fatty acids and antioxidants. Food Reviews International.

Dawczynski, C., Dittrich, M., Neumann, T., Goetze, K., Welzel, A., Oelzner, P., Volker, S., Schaible, A.M., Troisi, F., Thomas, L., Pace, S., Koeberle, A., Werz, O., Schlattmann, P., Lorkowski, S., Jahreis, G., 2018. Docosahexaenoic acid in the treatment of rheumatoid arthritis: A double-blind, placebo-controlled, randomized cross-over study with microalgae vs. sunflower oil. Clinical Nutrition 37, 494-504.

de Castro, G.S., Andrade, M.F., Pinto, F.C.S., Faiad, J.Z., Seelaender, M., 2022. Omega-3 Fatty Acid Supplementation and Its Impact on Systemic Inflammation and Body Weight in Patients With Cancer Cachexia-A Systematic Review and Meta-Analysis. Frontiers in Nutrition 8.

de la Guia-galipienso, F., Martinez-Ferran, M., Vallecillo, N., Lavie, C.J., Sanchis-Gomar, F.,

Pareja-Galeano, H., 2021. Vitamin D and cardiovascular health. Clinical Nutrition 40, 2946-2957.

Franchi, C., Ardoino, I., Bosetti, C., Negri, E., Serraino, D., Crispo, A., Giacosa, A., Fattore, E., Dolci, A., Bravi, F., Turati, F., La Vecchia, C., D'Avanzo, B., 2022. Inverse Association between Canned Fish Consumption and Colorectal Cancer Risk: Analysis of Two Large Case-Control Studies. Nutrients 14.

Hansen, A.L., Ambroziak, G., Thornton, D., Dahl, L., Molde, H., Grung, B., 2020. Fatty Fish Intervention and Psychophysiological Responses to Mental Workload in Forensic Inpatients A Randomized Control Trial. Journal of Psychophysiology 34, 10-18.

Hsieh, S.L., Li, J.H., Dong, C.D., Chen, C.W., Wu, C.C., 2022. Carnosine suppresses human colorectal cancer cell proliferation by inducing necroptosis and autophagy and reducing angiogenesis. Oncology Letters 23.

Intarasirisawat, R., Benjakul, S., Visessanguan, W., 2011. Chemical compositions of the roes from skipjack, tongol and bonito. Food Chemistry 124, 1328-1334.

Jiang, W., Li, F.R., Yang, H.H., Chen, G.C., Hua, Y.F., 2021. Relationship Between Fish Oil Use and Incidence of Primary Liver Cancer: Findings From a Population-Based Prospective Cohort Study. Frontiers in Nutrition 8.

Laumann, R.D., Iversen, T., Frandsen, T.L., Molgaard, C., Stark, K.D., Schmiegelow, K., Lauritzen, L., 2022. Whole blood long-chain n-3 fatty acids as a measure of fish oil compliance in children with acute lymphoblastic leukemia: a pilot study. Prostaglandins Leukotrienes and Essential Fatty Acids 177.

Lofvenborg, J.E., Andersson, T., Carlsson, P.O., Dorkhan, M., Groop, L., Martinell, M., Tuomi, T., Wolk, A., Carlsson, S., 2014. Fatty fish consumption and risk of latent autoimmune diabetes in adults. Nutrition & Diabetes 4.

Sikka, P., Behl, T., Sharma, S., Sehgal, A., Bhatia, S., Al-Harrasi, A., Singh, S., Sharma, N., Aleya, L., 2021. Exploring the therapeutic potential of omega-3 fatty acids in depression. Environmental Science and Pollution Research 28, 43021-43034.

Stasiewicz, B., Wadolowska, L., Biernacki, M., Slowinska, M.A., Stachowska, E., 2022. Dietary Fat Intake: Associations with Dietary Patterns and Postmenopausal Breast Cancer-A Case-Control Study. Cancers 14.

Wang, Y., Liu, K., Long, T.T., Long, J.Y., Li, Y., Li, J.Y., Cheng, L.M., 2022. Dietary fish and omega-3 polyunsaturated fatty acids intake and cancer survival: A systematic review and meta-analysis. Critical Reviews in Food Science and Nutrition.

Yonezawa, K., Kusumoto, Y., Kanchi, N., Kinoshita, H., Kanegae, S., Yamaguchi, N., Ozawa, H., 2020. Recent trends in mental illness and omega-3 fatty acids. Journal of Neural Transmission 127, 1491-1499.

Zhang, T., Wu, S.S., Xu, F.Y., Chang, J.P., Guo, Y.X., Zhou, Z.T., Xu, R.W., Wang, T.C., Wang, X.M., Wang, M.H., Qin, S.Y., Zhang, S.G., Li, J., 2022. The Association between Dietary Protein Intake and the Risk of Pancreatic Cancer: Evidence from 14 Publications. Nutrition and Cancer-an International Journal.

ISSN 1582-1021
e-ISSN 2668-4764
Edited by "AUREL VLAICU" University
Arad, Romania



10.62591/Scien.Tech.Bull-Chem.FoodSci.Eng.2021.18.06

**Edited by "AUREL VLAICU" University**
**Arad, Romania, 2021**